Bioactive Materials 22 (2023) 518–534

Contents lists available at ScienceDirect

Bioactive Materials

journal homepage: www.keaipublishing.com/en/journals/bioactive-materials

Fabricating 3-dimensional human brown adipose microtissues for transplantation studies

Ou Wang [a,b], Li Han [c], Haishuang Lin [a], Mingmei Tian [d], Shuyang Zhang [e], Bin Duan [f], Soonkyu Chung [g], Chi Zhang [h], Xiaojun Lian [c], Yong Wang [c], Yuguo Lei [a,c,i,*]

[a] Department of Chemical and Biomolecular Engineering, University of Nebraska-Lincoln, NE, USA
[b] Biomedical Engineering Program, University of Nebraska-Lincoln, NE, USA
[c] Department of Biomedical Engineering, Pennsylvania State University, PA, USA
[d] China Novartis Institutes for BioMedical Research Co., Ltd., Beijing, China
[e] Department of Chemistry, University of Nebraska-Lincoln, NE, USA
[f] Mary & Dick Holland Regenerative Medicine Program and Division of Cardiology, Department of Internal Medicine, University of Nebraska Medical Center, Omaha, NE, USA
[g] Department of Nutrition, University of Massachusetts, Amherst, MA, USA
[h] School of Biological Science, University of Nebraska-Lincoln, NE, USA
[i] Huck Institutes of the Life Sciences, Pennsylvania State University, PA, USA

ARTICLE INFO

Keywords:
Brown adipocyte
Microtissue
Transplantation
Obesity
Type 2 diabetes

ABSTRACT

Transplanting cell cultured brown adipocytes (BAs) represents a promising approach to prevent and treat obesity (OB) and its associated metabolic disorders, including type 2 diabetes mellitus (T2DM). However, transplanted BAs have a very low survival rate in vivo. The enzymatic dissociation during the harvest of fully differentiated BAs also loses significant cells. There is a critical need for novel methods that can avoid cell death during cell preparation, transplantation, and in vivo. Here, we reported that preparing BAs as injectable microtissues could overcome the problem. We found that 3D culture promoted BA differentiation and UCP-1 expression, and the optimal initial cell aggregate size was 100 μm. The microtissues could be produced at large scales via 3D suspension assisted with a PEG hydrogel and could be cryopreserved. Fabricated microtissues could survive in vivo for long term. They alleviated body weight and fat gain and improved glucose tolerance and insulin sensitivity in high-fat diet (HFD)-induced OB and T2DM mice. Transplanted microtissues impacted multiple organs, secreted protein factors, and influenced the secretion of endogenous adipokines. To our best knowledge, this is the first report on fabricating human BA microtissues and showing their safety and efficacy in T2DM mice. The proposal of transplanting fabricated BA microtissues, the microtissue fabrication method, and the demonstration of efficacy in T2DM mice are all new. Our results show that engineered 3D human BA microtissues have considerable advantages in product scalability, storage, purity, safety, dosage, survival, and efficacy.

1. Introduction

According to World Health Organization data, about 10% of adults have obesity (OB), and the population with OB-associated type 2 diabetes mellitus (T2DM) will reach 300 million by 2025 [1]. Currently, no safe and long-lasting approaches exist to prevent/treat OB and T2DM [2]. Healthy humans have a substantial amount of brown adipose tissue (BAT), a tissue that can augment the whole-body energy expenditure [3–8]. Large clinical data shows BAT activity inversely correlates to body mass index, plasma glucose, and triglycerides levels, insulin resistance. BAT activity is a negative predictor of T2DM, dyslipidemia, coronary artery disease, cerebrovascular disease, congestive heart failure, and hypertension [3–8]. Furthermore, the beneficial effects of BAT are more pronounced in obese individuals, suggesting the importance of this tissue for the obese population [3–8]. Clinical studies have shown that augmenting BAT activities using pharmaceuticals (e.g., mirabegron [9], glucocorticoids [10], BIBO3304 [11]), or cold stimulation [12–15] enhances the whole-body energy expenditure, glucose tolerance, and

Peer review under responsibility of KeAi Communications Co., Ltd.
* Corresponding author. The Pennsylvania State University, PA, USA.
E-mail address: yxl6034@psu.edu (Y. Lei).

https://doi.org/10.1016/j.bioactmat.2022.10.022
Received 15 February 2022; Received in revised form 6 October 2022; Accepted 18 October 2022

insulin sensitivity [16–18]. These findings suggest that BAT is a promising therapeutic target. However, these BAT-activating approaches require sustained treatments, have significant side effects [19], and may not work for long term. Additionally, they may work poorly on patients with a low abundance of BAT, such as obese and aged individuals.

An alternative approach that can overcome these problems is to augment BAT mass and activity via tissue or cell transplantation. Several groups transplanted three-dimensional (3D) BAT (0.1–0.2 g) obtained from healthy mouse donors to diet-induced or genetically obese mice [20–23]. The transplantation significantly reduced plasma glucose, triglyceride, lipid levels, body weight gain, fat composition, and hepatic steatosis [22,23] while increasing the body energy expenditure, oxygen consumption rate (OCR), glucose homeostasis, and insulin sensitivity [24,25]. Transplanted BAT could directly burn fatty acids and glucose and dissipate the energy as heat via nonshivering thermogenesis (e.g., act as an energy sink) [18,19]. They also secreted soluble factors and exosomes that enhanced glucose uptake and energy expenditure in the heart, muscle, and white adipose tissue (WAT) (e.g., act as an endocrine organ) [16,26–30]. These pre-clinical data show that BAT transplantation is a promising way to prevent and treat OB and its associated metabolic disorders. Although few studies have used T2DM mice as recipients, research found that transplanting mouse BAT into Streptozotocin (STZ)-induced diabetic mice prevented and reversed type 1 diabetes mellitus (T1DM) [24,31].

To date, most transplantation studies used mouse BAT since human BAT is located in deep organs, e.g., the supraclavicular, perirenal/adrenal, and paravertebral regions, and isolating sufficient human BAT for transplantation and research is challenging [32,33]. Thus transplanting human brown adipocytes (BAs) prepared via in vitro cell culture is necessary. Researchers recently isolated and immortalized human brown adipocyte progenitors (BAPs) and showed they could be efficiently expanded and differentiated into functional BAs in vitro [32,33]. When transplanted along with Matrigel, these BAPs could mature into functional BAs in vivo and prevent/reverse diet-induced OB and metabolic disorders [34]. Additionally, a few research groups successfully differentiated human pluripotent stem cells (hPSCs) into BAs and showed they were metabolically active in vitro and in mice models [35–43]. Thus both primary BAPs and hPSCs can be used as sources to prepare functional BAs for transplantation.

A critical challenge of transplanting in vitro prepared BAs is their low survival rate in vivo. A recent study showed that only 2.7% of mature BA (differentiated from immortalized mouse BAPs in vitro) were live in SCID mice 7 days after transplantation with Matrigel [21]. Consequently, BAs showed no efficacy in vivo [21]. We also found that the enzymatic dissociation during the harvest of the fully differentiated BAs cultured in the conventional 2D cell culture dishes killed many cells. To improve the survival rate during cell preparation, transplantation, and in vivo, most published studies transplanted BAPs and let these cells mature into functional BAs in vivo. For instance, the same study found that 12.1% of immortalized mouse BAPs survived 7 days after transplantation with Matrigel [21]. It should be noted that although the survival rate was improved, a 12.1% rate was still low. However, there are significant concerns with transplanting BAPs. First, the differentiation efficiency in vivo is typically low, and a large percentage of transplanted BAPs become non-BA cells, raising safety concerns [21]. Second, a large number of BAPs are typically injected to compensate for the low differentiation efficiency and survival rate. For instance, the Tseng study transplanted 1.5-2x10^7 BAPs per animal [34]. About 1.5-2x10^{10} BAPs would be needed for a human, considering the human body volume is about 1000 times of mouse body volume. This will make the cost of goods very high. Third, BAPs are still proliferating and have a tissue overgrowth risk, especially for immortalized cells. Lastly, researchers typically inject BAPs with Matrigel to restrict the cells at the transplantation site and enhance their survival [21]. However, Matrigel is extracted from mouse tumor tissue. It is not chemically defined and not compatible with clinical applications.

In short, transplanting BAPs is not an ideal approach. Transplanting fully differentiated BAs has advantages in that they can be prepared in vitro at high purity (e.g., ~93% in this study). They are less likely to have uncontrolled growth in vivo since they already exit the cell cycle. However, approaches must be developed to improve their survival rate in vivo and avoid cell death during cell harvest and transplantation in vitro. We propose that preparing BAs as injectable 3D microtissues can overcome these problems. Here, we report the BA microtissue fabrication method, their survival, safety, and capability to improve glucose and insulin homeostasis and manage body weight gain in HFD-induced OB and T2DM mice. Our results show that engineered 3D human BA microtissues have considerable advantages in product scalability, storage, purity, safety, dosage, survival, and efficacy.

2. Methods

2.1. 2D cell culture and differentiation

Immortalized BAPs are gifts from Dr. Tseng at Harvard University [32,33]. We followed published methods to culture and differentiate BAPs [32,33]. Briefly, BAPs were cultured in Dulbecco's Modified Eagle Media (DMEM, HyClone, #SH30003.03) supplemented with 10% FBS (Atlanta biologicals, #S11150). When cells reached 80% confluence, they were passaged (1:3) with 0.25% trypsin-EDTA (Giboco, #25200056). To induce differentiation, BAPs were seeded at 0.5×10^4 cells/cm^2 and maintained in the growth media to reach confluence. Then cells were cultured in differentiation media I consisting EBM-2 (Lonza, #CC-3156), 0.1% FBS, 5 μM SB431542 (Selleckchem, #S1067), 25.5 μg/ml ascorbic acid (Sigma, #A89605G), 4 μg/ml hydrocortisone (Sigma, #H0396), 10 ng/ml Epidermal Growth Factor (Peprotech, # 100-15), 0.2 nM 3,3′,5-Triiodo-L-thyronine (T3, Sigma, #T2877), 170 nM insulin (Sigma, #I9287-5 ML), 1 μM rosiglitazone (Sigma, #R2408), 0.5 mM 3-Isobutyl-1-methylxanthine (IBMX, Sigma, #I5879) and 0.25 μM dexamethasone (Sigma, #D4902) for 3 days, then in differentiation media II (differentiation media I without IBMX and dexamethasone) with media change once a week. Mature BAs could be obtained 20–30 days after induction.

2.2. Fabricating 3D BA microtissues

Aggrewells (Stemcell Technologies #34815, #34425) were pretreated with an anti-adherence rinsing solution (Stemcell Technologies, #07010) following the manufacturer's instruction. Single BAPs were seeded into Aggrewells with differentiation media I. Differentiation media II was used after three days and refreshed once a week. Differentiated BA microtissues were collected by centrifugation at 100*g* for 3 min. To prepare 3D BA microtissues in shaking plates, single BAPs were suspended in differentiation media I in a low adhesion 6-well plate (Corning, #3471) shaking at 75 rpm. Detailed methods of culturing cells in shaking plates can be found in our previous publications [44–48]. Differentiation media II was used after three days and refreshed once a week. The plate was tilted and placed in static for 5 min to settle down the microtissues to change the media. 90% of the exhausted media was replaced with fresh media. BA microtissues were collected by pipetting the media up and down to suspend the microtissues and spinning at 100 g for 3 min.

To prepare 3D BA microtissues in thermoreversible hydrogels, single BAPs were suspended in growth media I in low adhesion 6-well plate shaking at 75 rpm overnight to form BAP spheres. The spheres were then mixed with 10% ice-cold PNIPAAm-PEG (Cosmo Bio, #MBG-PMW20-5005) solution dissolved in DMEM media. The mixture was then cast on a tissue culture plate and incubated at 37 °C for 10 min to form a hydrogel before adding the pre-warmed differentiation media I. Differentiation media II was used after three days and refreshed once a week. To harvest BA microtissues, the media was removed, and ice-cold DPBS (Life Technologies, #21600044) was added to dissolve the hydrogel for

5 min. Finally, BA microtissues were collected by spinning at 100 g for 3 min. Detailed methods of encapsulating cells in this thermoreversible hydrogel can be found in our previous publications [44,48–52].

The prepared BAs were characterized for glucose uptake. WAs were used as controls. Methods to prepare WAs from WAPs were described in our previous publication [53]. Briefly, the differentiated BA and WA were incubated with serum-free DMEM containing 1 g/L D-(+)-glucose and 20 pM human insulin for 24 h before the glucose uptake test. Cells were incubated with HBSS buffer for 10 min before adding 4 nM of [^{3}H]-2-deoxyglucose. The [^{3}H]-associated radioactivity was measured by a liquid scintillation counter over 90 min.

To characterize the oxygen consumption rate (OCR), day 17 BA microtissues were treated with 0.25% trypsin-EDTA, dissociated into single cells plus small cell clusters, and plated to the Seahorse microplate. Cells were cultured for 7 more days before testing. The oxygen concentration in the cells was measured by XF24 extracellular flux analyzer (Seahorse) as described previously [53]. Briefly, oligomycin (1 μM) was added to measure the ATP turnover. Carbonyl cyanide 4-trifluoromethoxy phenylhydrazone (0.3 μM) was added to measure the maximum respiratory capacity. The mitochondrial respiration was blocked by 1 μM antimycin A and 1 μM rotenone. The OCR was presented by plotting the oxygen concentration in the medium as a function of time (pmol O_2/min).

For the qPCR measurement, total RNA was extracted using TRIzol reagent (Life Technologies), and 1 μg of RNA was reverse transcribed by iScript (Biorad). Gene expression was determined by real-time qPCR (Quant Studio 6 Flex Real-Time PCR, Applied Biosystems) using SYBR green (Fisher Scientific), and relative gene expression was determined based on the $2^{-\Delta\Delta CT}$ method with normalization of the raw data to *18S*. All primer sequences are available in Supplemental Table S1.

2.3. 3D microtissues transplantation studies

The animal experiments were conducted following the protocols approved by the University of Nebraska–Lincoln Animal Care and Use Committee. 6 mice were used for each study group. 6-week-old male B6.129S7-Rag1tm1Mom/J or Rag1 knock-out mice (Rag1$^{-/-}$) were purchased from Jackson. Mice were transplanted with 1.25 million cells suspended in DPBS (Rag1$^{-/-}$ HFD+BAT). Mice transplanted with DPBS were used as a sham control (Rag1$^{-/-}$ HFD+DPBS). Briefly, 3D microtissues were collected and transferred into a sample loading tip bent to have a U-shape. The tips were connected to a PE50 tube (BD Diagnostics system, #427516), and microtissues were slowly pushed into the center of the tube using a pipetman. The PE50 tube with microtissues was then bent into U-shape and placed into a microcentrifuge tube with both the PE50 tube ends kinked and facing up. The EP tube was centrifuged at 1000 rpm for 10 s to pack the microtissues tightly so that the media was located at the two ends. The PE50 tube was connected to a loading tip again. Microtissues were slowly pushed to one end of the PE50 tube using a pipetman. This operation removed the media so that no media was injected into the kidney capsule.

The right kidney of an anesthetized mouse was exposed. A small scratch on the flank of the kidney was made by a 25-gauge needle, creating a nick in the kidney capsule. Saline was applied with a cotton swab to keep the kidney wet. The PE50 tube was inserted into the capsule to make a small pocket under the capsule. Microtissues were slowly pushed into the pocket. The PE50 tube was carefully retracted, and the nick was cauterized with low heat. After stopping the bleeding, saline was applied, and the kidney was placed back. Details can be found in previous publications [54,55]. After 18 days of transplantation surgery, Rag1$^{-/-}$ mice without BA transplantation were fed with a normal chow diet or NCD. (Research diets, #D12450Ji) or HFD. (Research diets, #D12492i) and labeled as Rag1$^{-/-}$ NCD and Rag1$^{-/-}$ HFD, respectively. Rag1$^{-/-}$ mice transplanted with BA microtissues were fed with HFD and labeled Rag1$^{-/-}$ HFD+BAT. Wild-type (WT) mice without BA transplantation were fed with NCD or HFD and labeled as WT NCD and WT HFD.

Blood samples were collected from the mouse tail regularly to measure glucose concentrations. Cells were removed via centrifugation at 3000*g* for 10 min at 4 °C. The supernatant was transferred into a new tube and centrifuged at 3000 g for 5 min at 4 °C to collect the serum. Mouse fat and lean mass were analyzed by Minispec LF50 (Bruker, USA). For the glucose tolerance test (GTT), mice were fasted overnight for 16 h. Glucose (0.75 g/kg body weight) was administrated via intraperitoneal injection. Blood samples were collected to measure the glucose level at 0 (baseline), 30, 60, 90, and 120 min after injection. For the insulin tolerance test (ITT), mice were fasted in the morning for 8 h. Insulin (Sigma, #I9278-5 ML, 0.75 U/kg body weight) was administered via intraperitoneal injection. Blood samples were collected to measure the glucose level at 0 (baseline), 30, 60, and 90 min after injection.

2.4. Immunocytochemistry

Cells cultured on 2D were fixed with 4% paraformaldehyde (PFA) at room temperature for 15 min, permeabilized with 0.25% Triton X-100 for 10 min, and blocked with 5% donkey serum for 1 h before incubating with primary antibodies (Table S2) in DPBS + 0.25% Triton X-100 + 5% donkey serum at 4 °C overnight. After washing, secondary antibodies (Table S2) were added and incubated at room temperature for 2 h, followed by incubating with 10 mM 4′,6-Diamidino-2-Phenylindole, Dihydrochloride (DAPI) for 10 min. Cells were washed with DPBS three times before imaging with a Fluorescent Microscopy (Zeiss, Germany). For 3D microtissues immunostaining, microtissues were fixed with 4% PFA at 4 °C overnight. 40 μm thick tissue sections were obtained via cryosection. The sections were washed with DPBS three times and stained as the 2D cell cultures.

For in vivo studies, mouse tissues were harvested and fixed with 4% PFA at 4 °C overnight. 5 μm thick sections were obtained via paraffin embedding and section. The sections were deparaffined with xylene three times and rehydrated sequentially in 100%, 95%, 70%, 50% ethanol, and distilled water. For hematoxylin and eosin (H&E) staining, rehydrated sections were stained in Mayers Hematoxylin (Ricca Chemical Company, #3530-16) for 1 min, washed in distill water for 5 times, in DPBS once, and in distilled water 3 times with 1 min for each wash and stained in Eosin (Fisher, #SE23-500D) for 1 min. The sections were then dehydrated in 95% ethanol (3 times), 100% ethanol (2 times), and xylene (3 times) with 1 min for each wash before being mounted with coverslips. For immunostaining, heat-induced epitope retrieval was done on rehydrated tissue sections using the antigen retrieval buffer (Abcam, #ab93680) following the manufacturer's instruction. The sections were stained as the 2D cell cultures.

For flow cytometry, microtissues were dissociated into single cells with 0.25% trypsin-EDTA. Single cells were fixed with 4% PFA and stained with primary antibodies at 4 °C overnight. After washing (three times) with 1% BSA in DPBS, secondary antibodies were added and incubated at room temperature for 2 h. Finally, cells were washed with 1% BSA in DPBS and analyzed using CytoFLEX LX (Beckman Coulter, U. S.A.). Isotype controls served for negative gating.

To measure the plasma cytokines using mouse adipokine array and human obesity array, mice were sacrificed. Blood was collected, and serum was isolated, as described above. Then, 100 μL serum was applied to the mouse adipokine array (R&D systems, #ARY-013) following the manufacturer's instruction. 70 μL serum was applied to the human obesity array (RayBiotech, #QAH-ADI-3-2) following the manufacturer's instructions.

2.5. Statistical analysis

The data are presented as the mean ± SEM Unpaired *t*-test and one-way analysis of variance (ANOVA) were used to compare two and more than two groups, respectively. Two-way ANOVA was used to compare mice metabolic curves and arrays. $P < 0.05$ was considered statistically

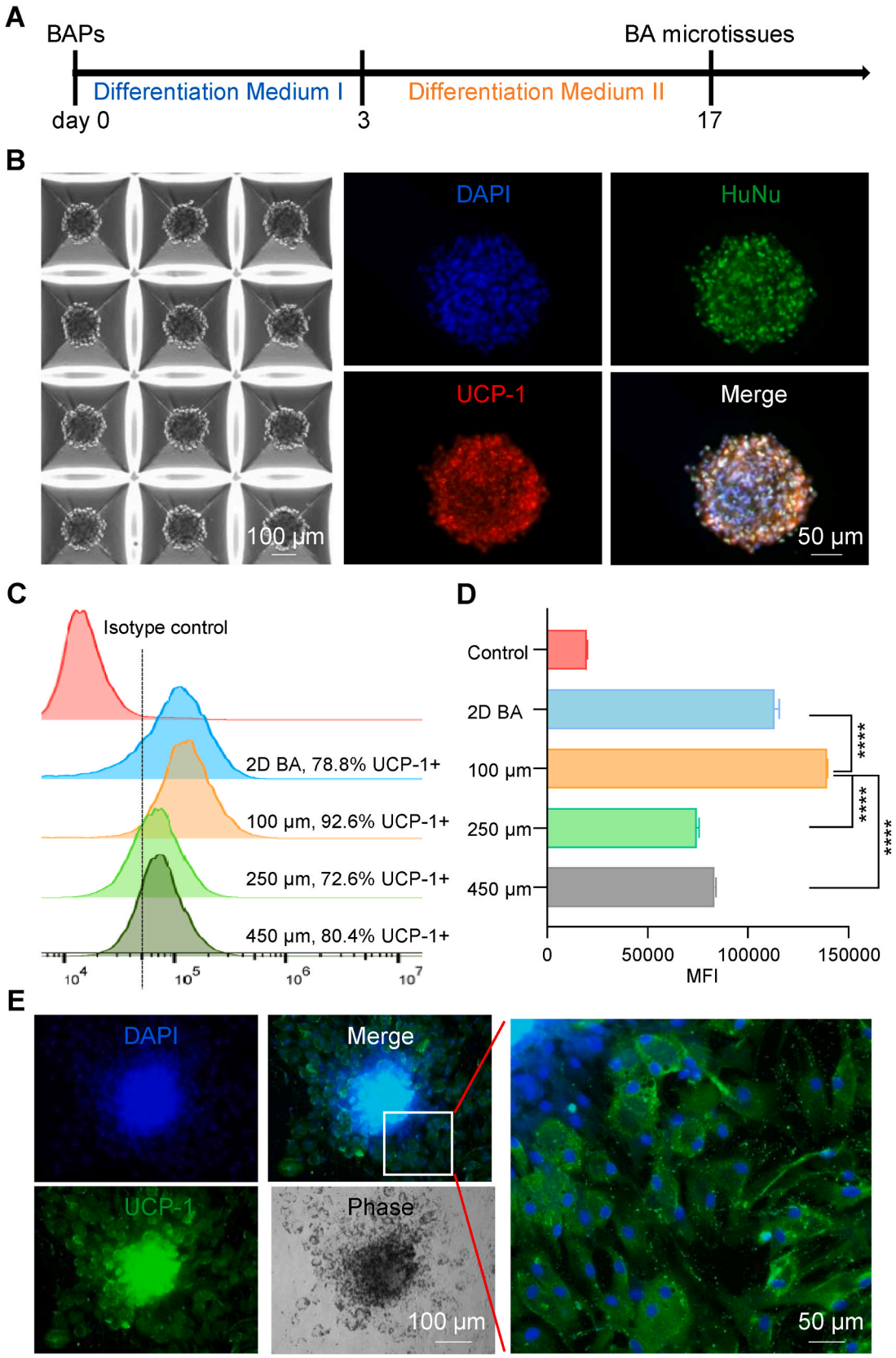

Fig. 1. 3D culture enhanced BA differentiation. (**A**) BA differentiation protocol. (**B**) 3D BA microtissues in microwells on day 17 and their immunostaining. HuNu: human nuclear antigen. (**C**) Flow cytometry analysis of UCP-1 expression on day 17 for BAs prepared in 2D culture and 3D culture with varied aggregate sizes. (**D**) The mean fluorescent intensity (MFI) of UCP-1 as measured with flow cytometry in (**C**). (**E**) The day 17 BA microtissues were plated on 2D surface for 6 days and stained for UCP-1 expression. Data are represented as mean ± SEM (n = 3). ****$p < 0.0001$.

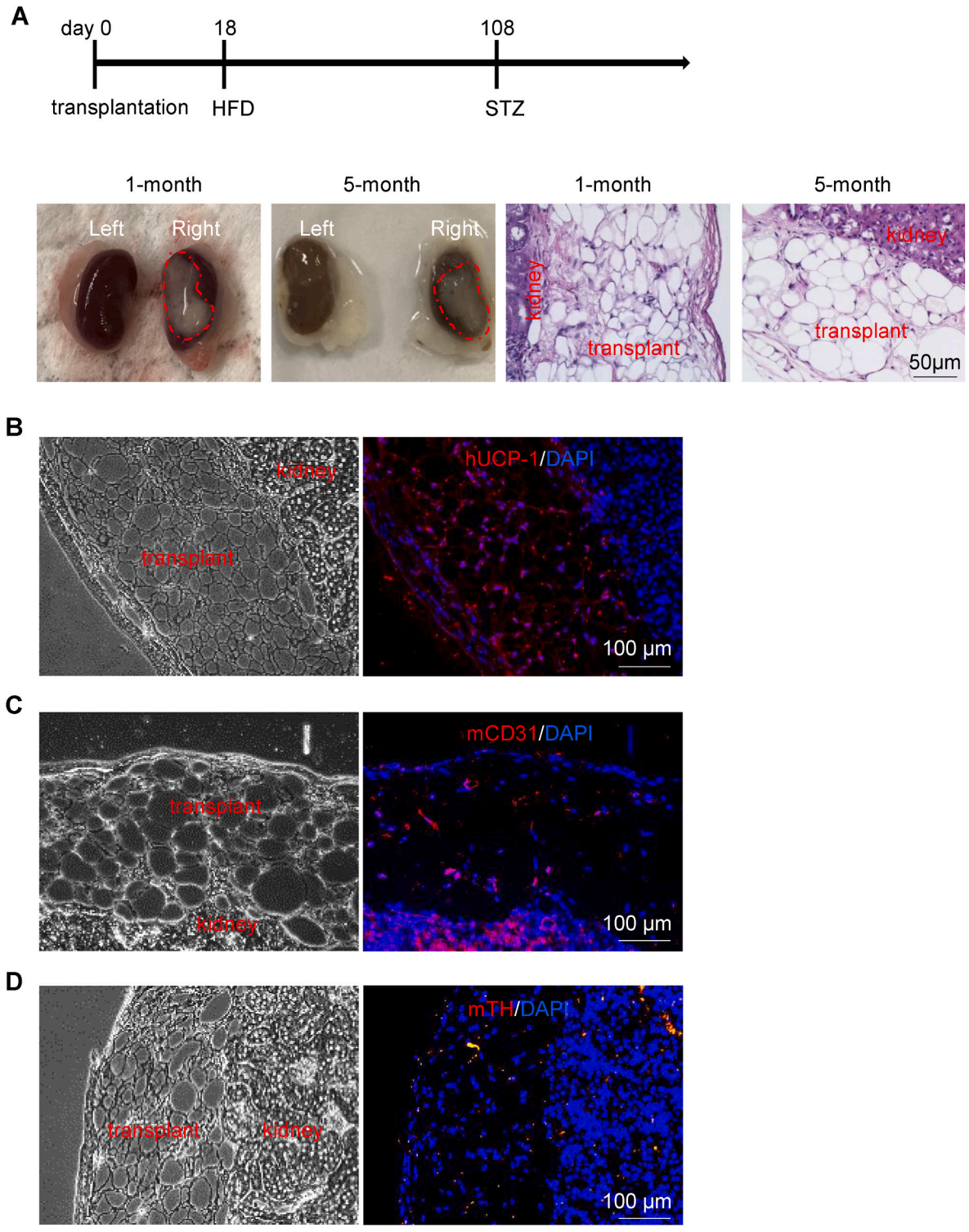

Fig. 2. BA microtissues survived in vivo. (**A**) The transplantation protocol. Photos and H&E staining of 1-month and 5-month transplants are shown. Only the right kidney had transplant. The transplants are outlined. The transplant and adjacent kidney tissue are labeled in H&E stain images. Immunostaining of the 5-month transplant and adjacent kidney tissue with human UCP1 (hUCP1) (**B**), mouse CD31 (mCD31) (**C**), and mouse tyrosine hydroxylase (mTH) (**D**).

significant.

3. Results

3.1. Fabricating 3D BA microtissues

The brown adipocyte progenitors (BAPs) used in this study were isolated from the superficial neck fat of a human subject and have been well characterized and documented [32,33]. We previously optimized a protocol to efficiently differentiate these BAPs into metabolically active BAs [53]. Given the intimate relationship between BAs and capillary networks in vivo, we pre-exposed BAPs to endothelial growth media (EGM) for 48 h before BA differentiation. The pre-exposure significantly promoted brown differentiation efficiency and metabolic activities. We

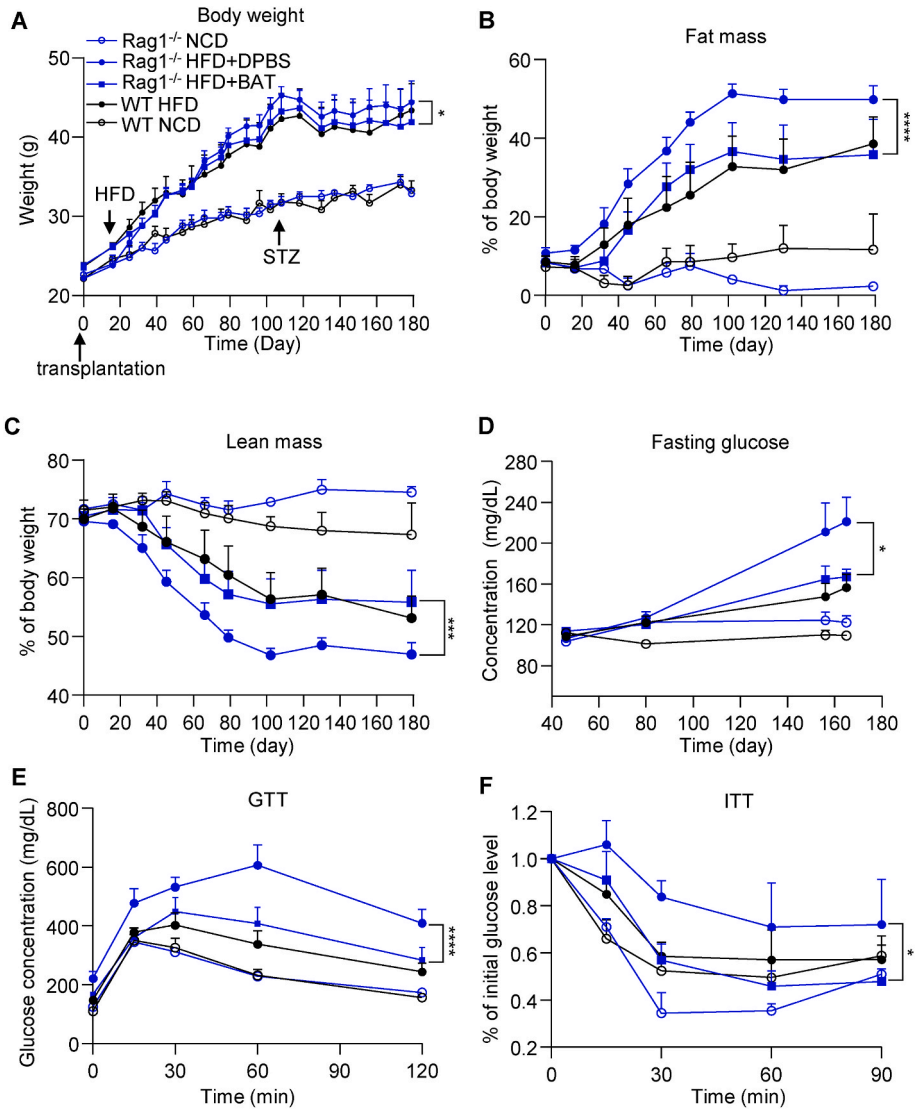

Fig. 3. BA microtissues alleviated obesity and diabetes. (**A**) Body weight gain, (**B**) % fat mass, (**C**) % lean mass, (**D**) fasting glucose level, (**E**) GTT (day 150), and (**F**) ITT (day 170). WT: wild type mouse; Rag1−/−: Rag1 knock-out mice; NCD: normal chow diet; HFD: high fat diet. BAT: brown adipose microtissues. Data are represented as mean ± SEM (n = 6). *p < 0.05, ***p < 0.001, ****p < 0.0001.

applied the same differentiation protocol to prepare BA microtissues in 3D. Single BAPs were placed in microwells (Aggrewells). Cells associated with each other, gradually contracted, and formed compact spheroids after 24 h (Fig. S1A). Like the 2D differentiation, we cultured the microtissues in differentiation media I for 3 days and then in differentiation media II with a media refresh every 7 days (Fig. 1A). Microtissues grew in size significantly during the differentiation (Fig. S1A). For instance, microtissues with an initial diameter of 100 μm became 200 μm on day 17 (Fig. S1A). The microtissue size growth can result from the cell number increase due to cell proliferation or the cell size increase, or both. Cell proliferation and size growth were observed during the differentiation of BAPs to BAs in 2D culture [56]. Immunostaining showed that most of the cells in the microtissues expressed the UCP-1 protein, a biomarker of mature and functional BAs (Fig. 1B). UCP-1 is a mitochondria membrane protein critical for nonshivering thermogenesis [57,58].

To study if the microtissue size influences the differentiation efficiency, we prepared microtissues with a diameter of 100, 250, and 450 μm (initial diameter) via seeding different numbers of cells and differentiated them. All microtissues grew in size significantly (Fig. S2). While the 100 and 250 μm microtissues maintained spherical, the 450 μm microtissues gradually became non-spherical (Fig. S2D). Cell death (Fig. S2D, red arrows) and fusion between microtissues (Fig. S2D, blue arrows) were observed only in the 450 μm microtissues. On day 17, flow cytometry analysis showed 92.6%, 72.6%, and 80.4% of the cells in the 100, 250, and 450 μm microtissues were UCP-1 positive. For comparison, 2D culture resulted in 78.8% UCP-1 positive cells (Fig. 1C). The mean fluorescent intensity (MFI) of UCP-1 intensity in 100 μm microtissues was significantly higher than in other groups (Fig. 1D).

When the day 17 microtissues were placed in a conventional tissue culture plate, they adhered to the surface, and individual cells migrated out (Fig. 1E, S1B, S1C). These cells had the classical BA characteristics. They expressed a high level of UCP-1 protein (Fig. 1C, 1D, 1E, S3D) and had multiple small oil droplets (Fig. 1E, S3A, S3B, S3C) and a high mitochondrial content (Fig. S3C). Furthermore, they expressed the typical BA marker genes at high levels (Fig. S3E). In addition, the differentiated BA showed a significantly higher glucose uptake and oxygen consumption rate compared to WA (Fig. S4). Our data show that i) BAP can be differentiated into BA in 3D to prepare BA microtissues; ii) a 3D microenvironment promotes brown adipogenesis and UCP-1 expression. However, a small microtissue size should be used to maximize the benefits.

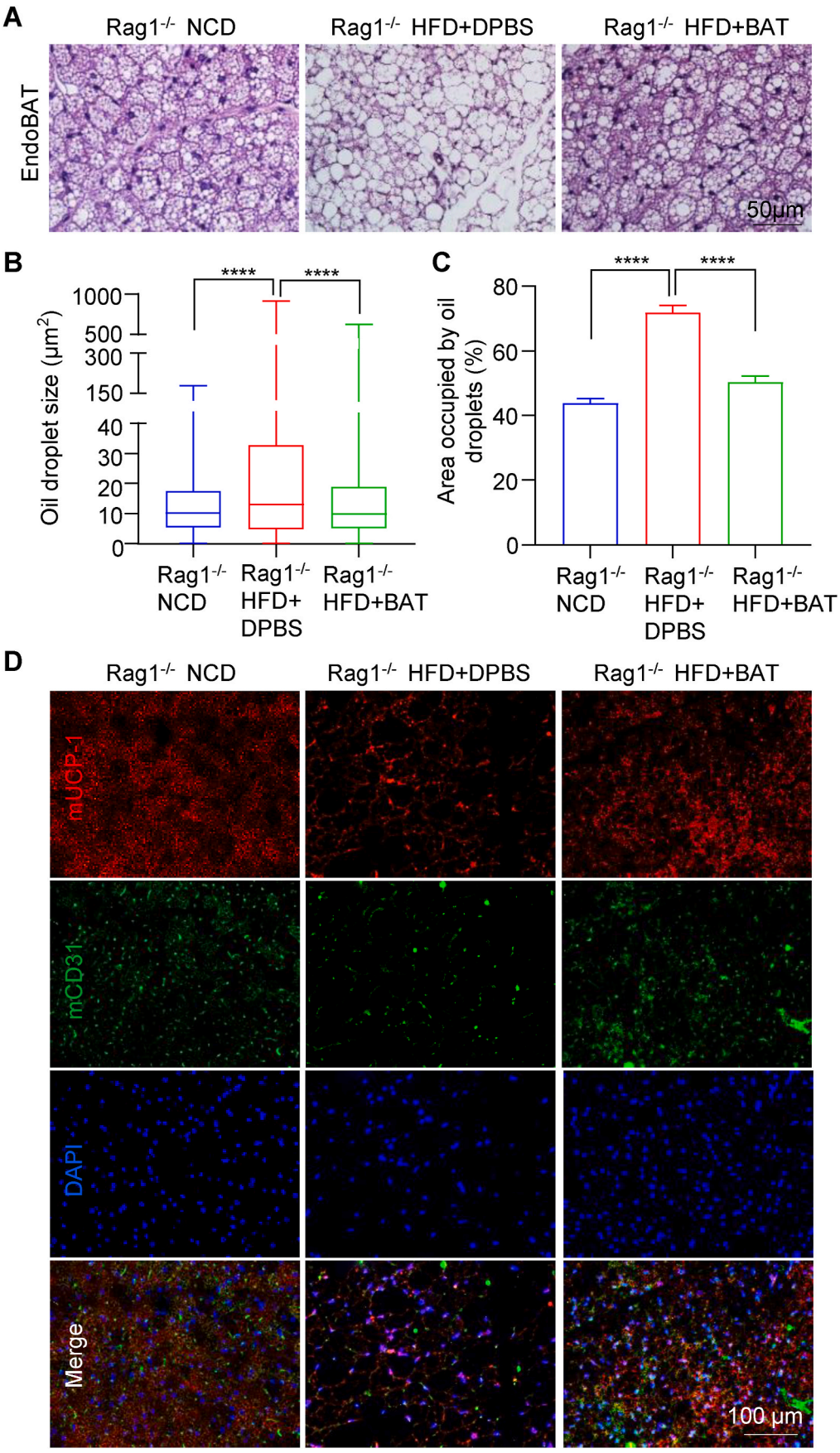

Fig. 4. BA microtissue transplants impacted endogenous BAT (endoBAT). (**A**) H&E staining of endoBAT. Oil droplet size (**B**) and area (**C**) in endoBAT. (**D**) Mouse UCP-1 and CD31 expression in endoBAT. (**E**) Mouse TH and CD31 expression in endoBAT. Data are represented as mean ± SEM (n = 6). ****$p < 0.0001$.

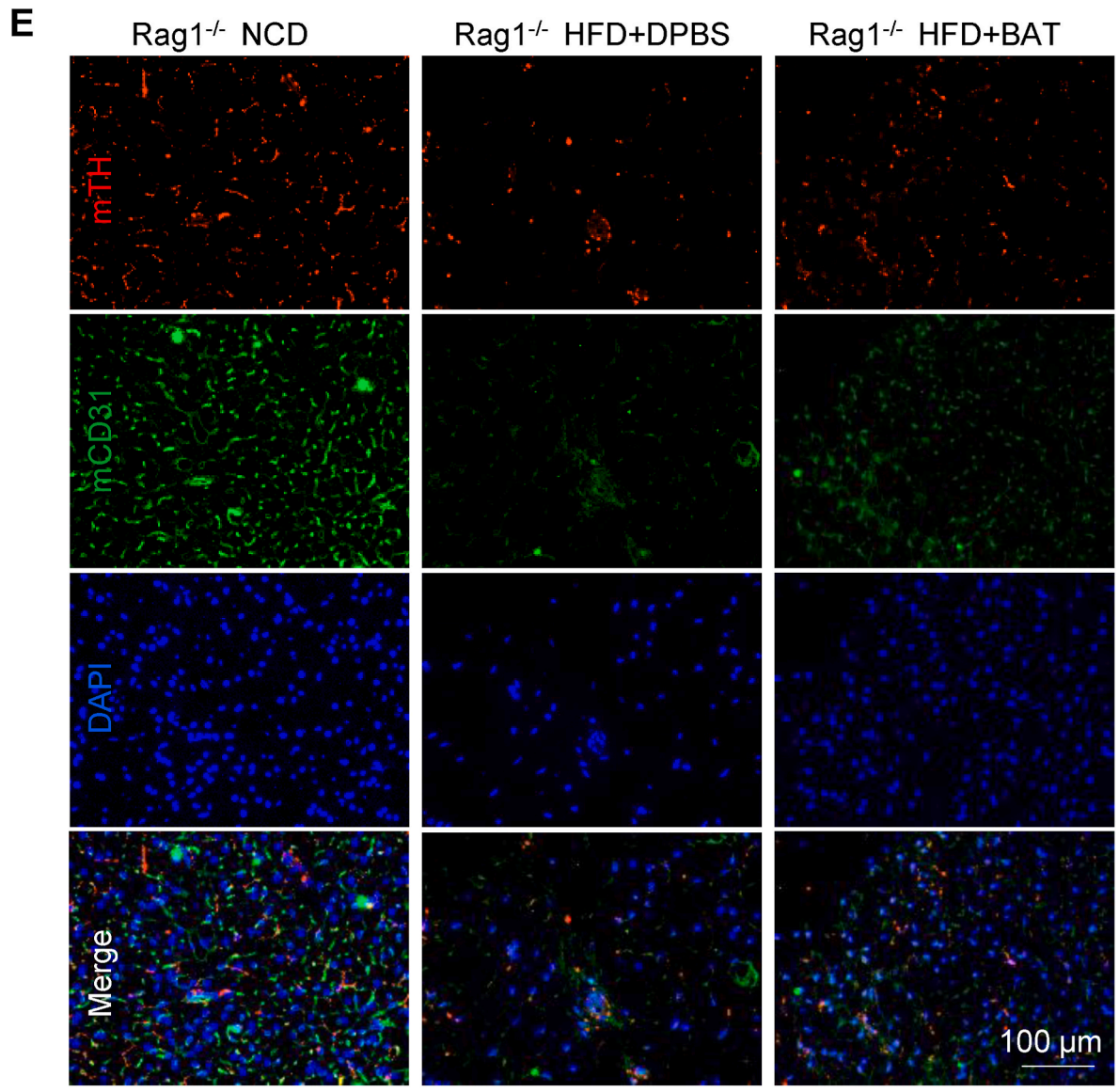

Fig. 4. (*continued*).

3.2. BA microtissue transplantation studies

Next, we studied if the 3D BA microtissue could be transplanted via injection and if they could survive and function in vivo. As said, very few BAT transplantation studies used T2DM mice. To fill the gap, we used a high-fat diet (HFD)-induced OB and T2DM mouse model to test the fabricated BA microtissues. We selected the immune-deficient Rag1$^{-/-}$ mice as recipients since they tolerate xenogeneic and allogeneic tissues and have HFD-induced OB and metabolic disorders [59,60]. In addition, they developed diabetes when given STZ [61]. Rag1$^{-/-}$ mice fed with a normal chow diet (NCD) and HFD with DPBS transplantation were used as positive and negative controls to evaluate the microtissue efficacy. WT mice fed with NCD and HFD were also included to assess the difference in response to HFD between WT and Rag1$^{-/-}$ mice. HFD was initiated 18 days post-transplantation. A significant number of adipose tissue was found in the kidney capsule 1 month and 5 months after transplantation (Fig. 2A). H&E staining showed the dense kidney tissue and the adjacent adipose tissue with large amounts of oil droplets (Fig. 2A). The oil droplets were bigger in the 5-month sample. No tumor or non-adipose tissues were found in the transplants, indicating the safety of fully differentiated BAs in vivo. We found that the oil droplets of the transplanted BAT were significantly bigger than those of the endoBAT of NCD-fed mice (Fig. 4A). A high level of UCP-1 protein was observed in the transplanted BAT (Fig. 2B). Host blood vessels grew into the transplants (Fig. 2C). The vessel density was comparable to the endoBAT of HFD mice but lower than the endoBAT of NCD mice (Fig. 4D). Innervation is critical for BA function [62]. Tyrosine hydroxylase (TH+) nerves were found in the transplants (Fig. 2D), and their density was comparable to the endoBAT of HFD mice but lower than the endoBAT of NCD mice (Fig. 4E).

We regularly measured the body weight, fat and lean mass, plasma glucose level, glucose tolerance, and insulin sensitivity (Fig. 3). To mimic the β cell dysfunction of T2DM, we injected low-dose STZ (90 mg/kg) after 3-month HFD. The body weight drops, and the fasting glucose level rise after the STZ injection, indicating the progression of T2DM (Fig. 3A and D). There was no significant difference in total diet intake between the HFD groups. Under HFD, both WT and Rag1$^{-/-}$ mice developed OB (Fig. 3A) and grew large fat masses (Fig. 3B and C). We found Rag1$^{-/-}$ mice were slightly more prone to HFD-induced OB and metabolic disorders but were suitable for our studies. The transplant significantly reduced the body weight gain, fat content, and fasting glucose level while increasing insulin sensitivity and glucose tolerance

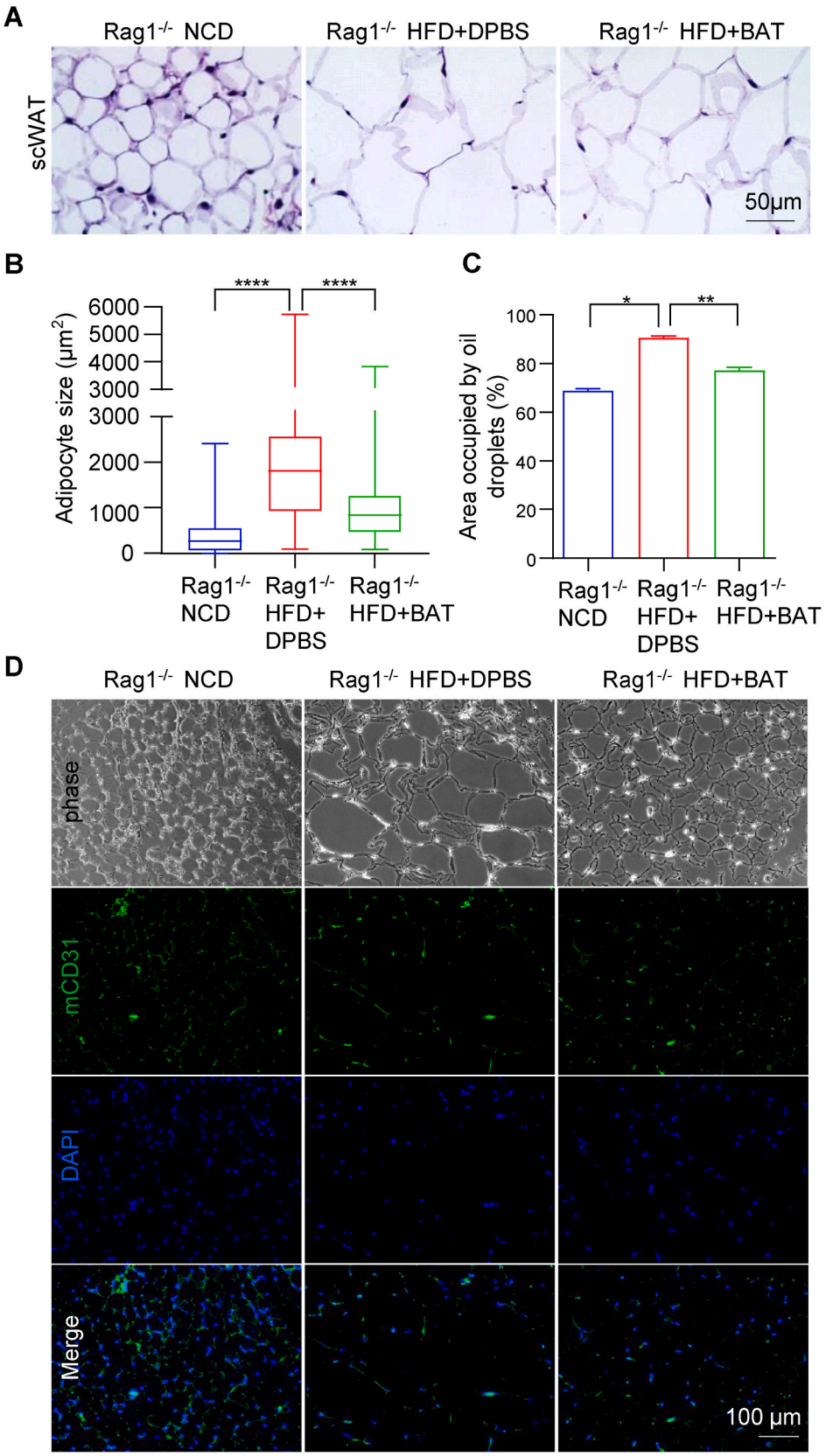

Fig. 5. BA microtissues reduced endogenous WAT hypertrophy and liver steatosis. (**A**) H&E staining of mouse subcutaneous white adipose tissue (scWAT). Adipose size (**B**) and area (**C**) in scWAT. (**D**) Mouse CD31 expression in scWAT. (**E**) H&E staining of mouse liver. (**F**) Adipose area in liver. Data are represented as mean ± SEM (n = 6). *p < 0.05, **p < 0.01, ****p < 0.0001.

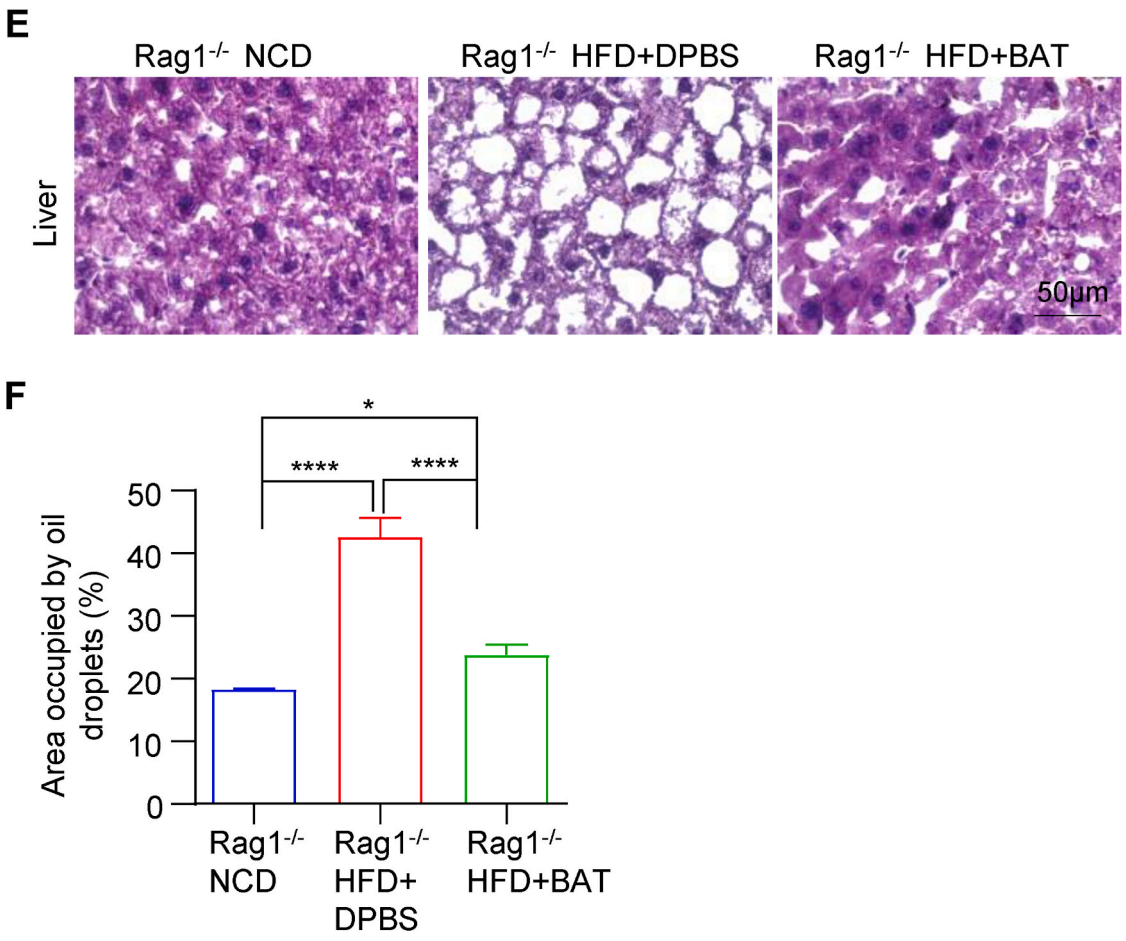

Fig. 5. (*continued*).

(Fig. 3). In summary, fabricated 3D BA microtissues were successfully injected into the kidney capsule, survived well, and maintained UCP-1 protein expression for at least 5 months. The transplants were effective in alleviating HFD-induced OB and metabolic syndrome.

3.3. BA microtissue transplants impacted multiple organs in vivo

We characterized the impact of the BA transplant on the morphology and structures of different mouse organs. For the endogenous BAT (endoBAT), HFD increased the size of oil droplets (Fig. 4A–C). The BA transplants prevented the increase. For instance, the areas occupied by oil droplets in NCD, HFD, and HFD plus BA transplantation mice were 43.8%, 71.9%, and 48.9%, respectively. The mean diameter of oil droplets were 8.6 μm, 12.4 μm, and 9.0 μm in NCD, HFD, and HFD plus BA transplantation mice, respectively. Compared to NCD mice, HFD mice had reduced mUCP-1 protein expression (Fig. 4D), blood vessel density (Fig. 4D and E), and TH+ nerve density (Fig. 4E). The transplanted BA microtissues significantly improved the mUCP-1 protein expression, blood vessel density, and TH+ nerve density in HFD mice. In general, HFD mice with BA microtissues had similar BA morphology, blood vessel, and nerve densities to the NCD mice.

The adipocyte size and oil droplets of subcutaneous WAT (scWAT) were increased by the HFD. BA microtissues significantly reduced these increases (Fig. 5A–C). The areas occupied by oil droplets in NCD, HFD, and HFD plus BA transplantation mice were 68.7%, 90.5%, and 77.1%, respectively. The mean diameter of adipocytes were 42.0 μm, 96.2 μm, and 70.6 μm in NCD, HFD, and HFD plus BA transplantation mice, respectively. CD31 staining showed fewer blood vessels in HFD-fed mice. BA microtissues increased the blood vessel density in HFD-fed mice (Fig. 5D). The liver fat content was significantly increased in HFD mice but was almost normalized by BA microtissues (Fig. 5E). The areas occupied by oil droplets in NCD, HFD, and HFD plus BA transplantation mice were 18.24%, 42.52%, and 23.76%, respectively. The results showed that the transplanted microtissues profoundly affected multiple organs.

We used a Human Obesity Antibody Array to measure human protein factors in the blood. We found that the concentrations of human adiponectin, chemerin, and TGF-β1 in mice with transplants were significantly higher than background (Fig. 6A), indicating the transplanted BAs were secreting soluble factors. Research has shown that adiponectin secreted by white and brown adipocytes has a protective role in obesity-associated metabolic and cardiovascular diseases. Adiponectin influences multiple tissues, such as the liver, skeletal muscle, and vascular system. Adiponectin can increase insulin sensitivity [63,64], suppress inflammation, and reduce atherosclerosis [65–67]. Plasma adiponectin level negatively correlates with obesity, and adiponectin deficiency enhances HFD-induced insulin resistance [68]. Chemerin plays a positive role in metabolic health [69,70]. TGF-β1 is a mediator of insulin resistance in metabolic disease [71,72]. We also used a Mouse Adipokine Antibody Array to measure 38 obesity-related mouse molecules. The levels of adiponectin, ANGPT-L3, C-reactive protein, ICAM-1, IGFBP-3, IGFBP-5, IGFBP-6, lipocalin-2, and pentraxion2 were significantly reduced, and the IGF-1 concentration was increased by the HFD. (Fig. 6B and C). The transplanted BA microtissues normalized all of these molecules (Fig. 6C). Thus, the transplanted microtissues significantly affected the expression levels of endogenous adipokines.

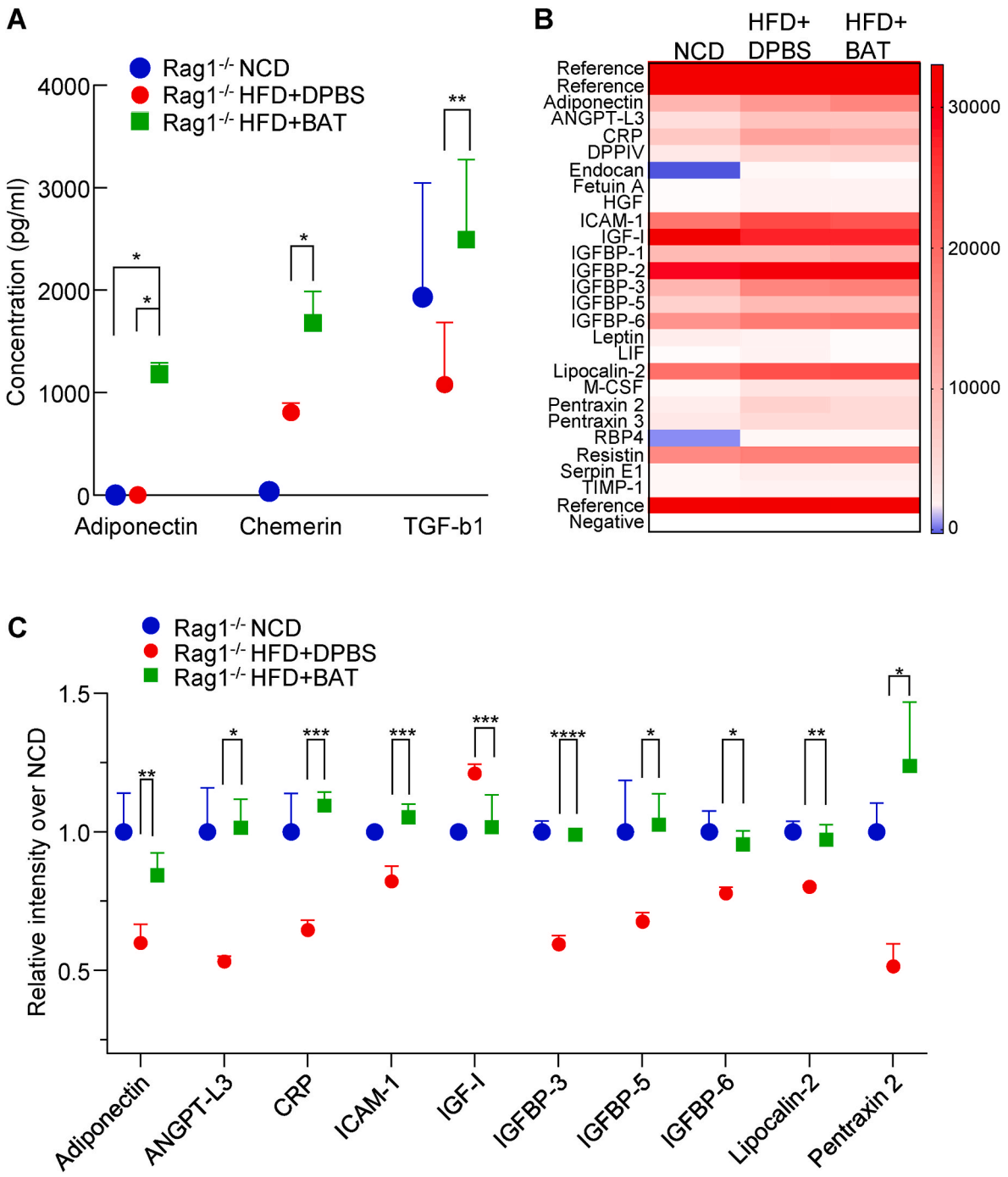

Fig. 6. BA microtissues secreted human protein factors and modulated endogenous adipokines. (**A**) Protein factors in mouse plasma detected using human obesity antibody array. (**B, C**) Heatmap and quantification of adipokines in mouse plasma detected using mouse adipokine antibody array. Data are represented as mean ± SEM (n = 3). *p < 0.05, **p < 0.01, ***p < 0.001, ****p < 0.0001.

3.4. Scale up BA microtissue production

Although microwells can produce microtissues with precisely controlled size, microwells are unsuitable for producing microtissues at large scales for future extensive animal studies, drug screens, and clinical applications. 3D suspension culturing, which suspends and cultures cells in an agitated media, has been extensively studied to scale up cell production due to its simplicity, easiness of scaling up, and automation [44,73–76]. We thus investigated if BA microtissues could be prepared in 3D suspension culture. We found single BAPs associated to form small uniform aggregates after 24 h. However, severe cell aggregation occurred after long-term culture (e.g., after day 4), resulting in aggregates with widely distributed size (Fig. 7A). The final volumetric cell yield was also low (e.g., $\leq 1 \times 10^6$ cells/mL). It is known that the mass transport in agglomerates >400 μm in diameter (the diffusion limit in human tissue) becomes insufficient, leading to cell growth arrest, apoptosis, and uncontrolled differentiation [74,77]. Thus, suspension culture alone has difficult to produce the BA microtissues at large scales.

A way to overcome the excessive cellular aggregation is to culture cells in a hydrogel scaffold. Hydrogels can act as physical barriers to eliminate excessive cell agglomeration and shear stress [78–81]. We previously found that single human pluripotent stem cells (hPSCs) could

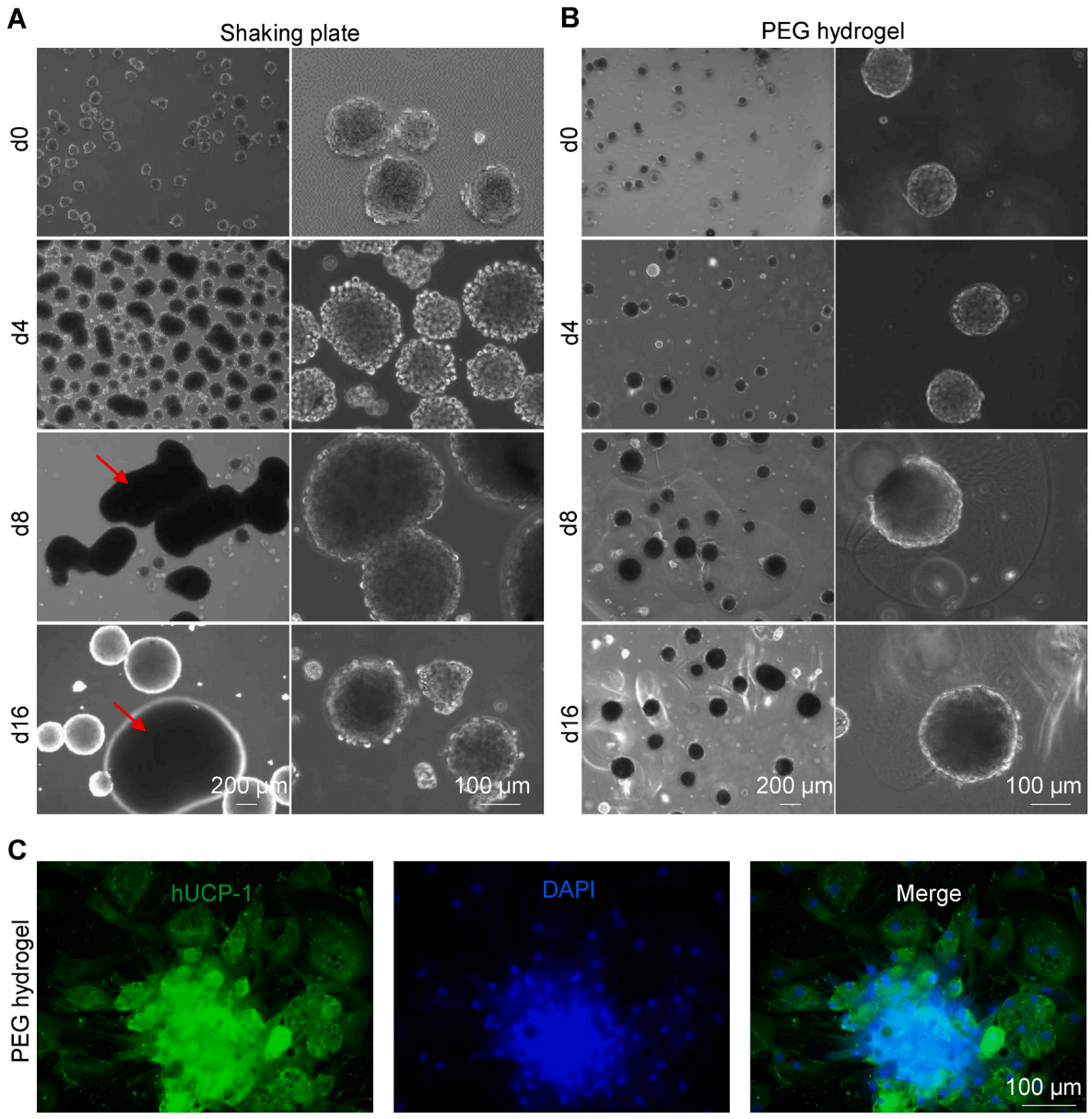

Fig. 7. Scaling up BA microtissue production. Preparing BA microtissues in shaking plates (**A**) and PEG hydrogel (**B**). (**C**)Immunostaining of day 17 BA microtissues prepared in PEG hydrogel. Microtissues were plated on 2D surface for 6 days before staining.

grow in a thermoreversible PNIPAAm-PEG hydrogel to generate large amounts of uniform hPSC spheroids [44,49,52,82–86]. We tried encapsulating single BAPs in the same hydrogel to grow BA microtissues. However, single BAPs did not expand in the hydrogel scaffold. We thus suspended single BAPs in 3D suspension culture for 24 h to generate small and uniform cell BAP aggregates as described in the above paragraph. These BAP aggregates were then encapsulated in the PNIPAAm-PEG hydrogel and cultured for 16 days with differentiation media to prepare BA microtissues. With this approach, we prepared large numbers of BA microtissues with well-controlled sizes (Fig. 7B). The final volumetric yield could reach 1×10^7 cells/mL hydrogel. In addition, the resultant BAs expressed a high level of UCP-1 protein (Fig. 7C). Thus, the combination of 1-day suspension culture and 16-day differentiation in PNIPAAm-PEG hydrogel can be used to scale up the microtissues production. Lastly, we evaluated if BA microtissues could be preserved. Microtissues preserved in cell culture media at room temperature for 24 h (Fig. 8B) had similar viability to the fresh sample (Fig. 8A). Microtissues could also be cryopreserved in liquid nitrogen for long-term without significantly sacrificing cell viability (Fig. 8C).

4. Discussion

Our study showed that human BAPs could be differentiated into mature BAs in 3D to prepare injectable BA microtissues (Fig. 1, S1, S2, S3). The 3D culture promoted BA differentiation and UCP-1 protein expression. The optimal initial BAP spheroid size is 100 μm. BA microtissues could survive in vivo for long-term (Fig. 2). They significantly reduced body weight and fat gain and improved glucose tolerance and insulin sensitivity in HFD-induced OB and T2DM mice (Fig. 3). The transplanted BA microtissues impacted multiple tissues such as endogenous BAT, WAT, and liver (Figs. 4 and 5). In addition, they secreted protein factors and influenced the secretion of endogenous adipokines (Fig. 6). These microtissues could be produced in large numbers using 3D suspension culture assisted with a thermoreversible PEG hydrogel (Fig. 7) and could be cryopreserved (Fig. 8). To our best knowledge, this is the first report on fabricating human BA microtissues and showing

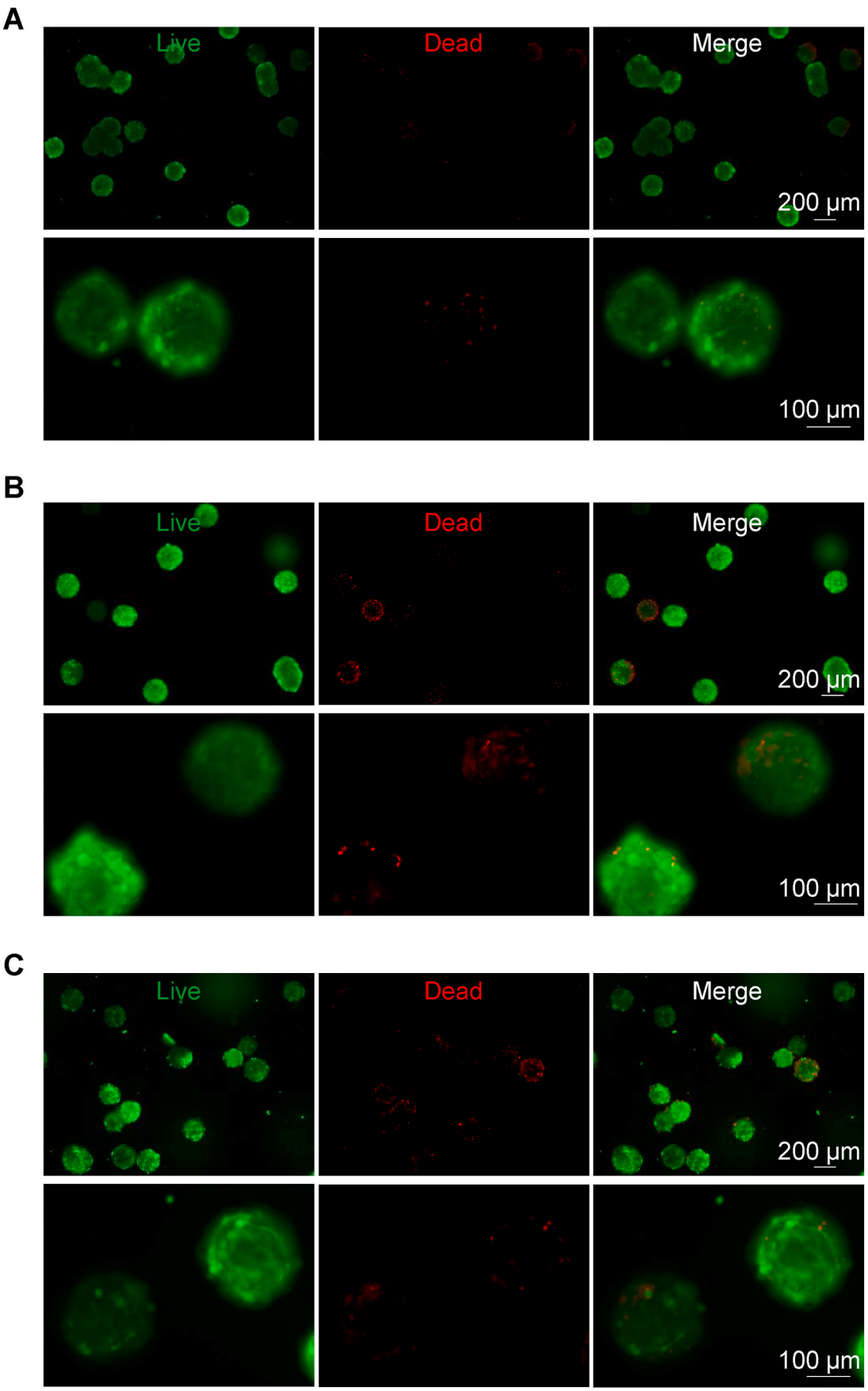

Fig. 8. Preserving BA microtissues. Live/dead cell staining of day 27 fresh BA microtissues (**A**), or stored at room temperature for 24 h (**B**), or stored in liquid nitrogen and recovered (**C**).

their safety and efficacy in OB and T2DM mice. The proposal of transplanting fabricated BA microtissues, the scalable microtissue fabrication method, the findings that 3D culture promotes BA differentiation and the microtissue size affects the differentiation, and the demonstration that BA transplantation is effective in T2DM mice are all new.

We found that the microtissue size significantly influenced the BA differentiation efficiency. The optimal diameter is about 100 μm (initial diameter). BAs have a high demand for glucose, oxygen, and nutrients to meet their high metabolic activities [21,87–91]. Nutrients are transported in these microtissues mainly through diffusion. Therefore, cells at the center of large microtissues may not have a sufficient supply of nutrients, negatively affecting the differentiation process. A second possible cause is that cells secrete autocrine or/and paracrine factors that are important to BA differentiation. The microtissue diameter influences the concentrations and gradients of these factors. The exact reason should be made clear in future studies.

We demonstrated that the production of BA microtissues could be scaled up using the 3D suspension culture to generate small BAP aggregates and followed by differentiating these aggregates in a 3D thermoreversible hydrogel matrix (Fig. 7). We recently developed a novel microbioreactor termed AlgTubes, in which cells are cultured in alginate hydrogel microtubes [45,46,92–97]. AlgTubes are scalable and have low costs. In addition, the cell aggregate size can be precisely controlled by the hydrogel tubes. AlgTubes can produce up to 5×10^8 cells per mL of culture volume. Future studies can apply AlgTubes to produce fibrous BA microtissues with uniform and precise size at high density.

BAT is among the most vascularized tissues in the body, averaging ~1.2 capillaries per BA (versus only ~0.4 capillaries per white adipocyte) [87–91]. A substantial blood supply is required to provide glucose, fatty acids, nutrients, and oxygen to fuel thermogenesis and rapidly distribute heat throughout the body [98]. Vascular cells also produce soluble and insoluble factors critical for BA functions and homeostasis; conversely, BAs produce a range of growth factors and cytokines that collectively modulate vascular growth, survival, remodeling, regression, and blood perfusion [89,91,99]. In obese mice, the capillary density in BAT decreases significantly (i.e., ~0.5 capillaries per BA), resulting in hypoxia and BAT degeneration [90]. We found that the transplanted microtissues gradually became white adipocyte-like in morphology (Fig. 2A), although UCP-1 proteins were still expressed at a high level (Fig. 2B). A potential reason for this whitening is the insufficient vascularization in the transplant. This agrees well with literature findings that the transplants had fewer blood vessels than endogenous BAT [21,100]. Consequently, BAs gradually decreased UCP-1 expression and became WAT-like features. There are two potential ways to address this problem. First, as shown in a published study [21], supplementing vascular endothelial growth factor (VEGF) to the transplant can significantly improve its engraftment, angiogenesis, and function. Second, endothelial cells can be included in the BA microtissues. As stated in the above paragraph, endothelial cells or vasculature are indispensable for BAT in vivo.

We used immortalized BAPs to prepare mature BA microtissues. No tumor or abnormal tissue growth was observed (Fig. 2), indicating that fully differentiated BAs are safe in vivo. Thus, it is applicable to isolate and immortalize BAPs from a patient and expand them to prepare BA microtissues for personalized BA augmentation therapy. An alternative approach is to prepare induced pluripotent stem cells (hiPSCs) for a patient. hiPSCs can be generated by reprogramming somatic cells [101–103]. They have unlimited proliferation capability and can be differentiated into all types of somatic cells. The transplant's immune rejection can also be avoided by preparing BAT from personalized hiPSCs [104,105]. Recent clinical studies showed that autologous hiPSCs-derived dopaminergic neurons and retinal cells were safe and effective in treating Parkinson's [106] and macular degeneration [105], respectively, indicating the coming of the hiPSCs-based personalized medicine era. Alternatively, universal hiPSCs can be engineered, for instance, via inactivating major histocompatibility complex (MHC) class I and II genes and overexpressing CD47 or/and PD-L1 [106–109]. The derivatives of universal hiPSCs are hypoimmunogenic and can be prepared at large scales as "off-the-shelf" allogeneic products. hiPSCs have been successfully differentiated into BAs that are metabolically active in vitro and in mice models [35–43]. Therefore, future studies can explore using hiPSCs to prepare BA microtissues.

Most published studies used obese [20–23] or T1DM mice [24,31] for BA transplantation. If BA transplantation can prevent/treat T2DM is still not well-known but is worthy of finding out, considering the sizeable T2DM patient population. We preliminarily showed that the transplanted BA microtissues alleviated HFD-induced body weight and fat tissue gain and improved glucose homeostasis and insulin sensitivity in HFD-fed T2DM mice (Fig. 3), showing the high potential of BA transplantation for preventing/treating T2DM. Previous transplantation studies found BAT transplants could work through two major mechanisms. They could directly burn fatty acids and glucose and dissipate the energy as heat [18,19] or secreted soluble factors to enhance glucose uptake and energy expenditure in the heart, muscle, and white adipose tissue or WAT [16,26–30]. We found that transplanted BA microtissues impacted the morphology and structure of the mouse organs (Figs. 4 and 5). They also secreted human cytokines and changed the expression levels of mouse cytokines in plasma (Fig. 6). These indicate that the second mechanism was active in the transplanted BA microtissues. Whether the transplants could function through the thermogenesis mechanism is unknown and should be investigated in the future.

5. Conclusion

Our study showed that 3D BA microtissues could be fabricated at large scales, cryopreserved for long term, and delivered via injection. BAs in the microtissues had higher purity and higher UCP-1 protein expression than BAs prepared via 2D culture. In addition, 3D BA microtissues had good in vivo survival and no uncontrolled tissue overgrowth. Furthermore, they showed good efficacy in preventing OB and T2DM with a very low dosage compared to literature studies. Our results show that fabricated 3D BA microtissues are promising anti-OB/T2DM therapeutics. They have considerable advantages over single BAs or BAPs in terms of product scalability, storage, purity, safety, dosage, survival, and efficacy.

Ethics approval

The animal experiments were conducted following the protocols approved by the University of Nebraska–Lincoln Animal Care and Use Committee.

CRediT authorship contribution statement

Ou Wang: Conceptualization, experiment design, experiment, Formal analysis, manuscript writing. **Li Han:** experiment, Formal analysis. **Haishuang Lin:** experiment, Formal analysis. **Mingmei Tian:** experiment, Formal analysis. **Shuyang Zhang:** experiment, Formal analysis. **Bin Duan:** Conceptualization, Formal analysis, manuscript revision. **Soonkyu Chung:** Conceptualization, Formal analysis, manuscript revision. **Chi Zhang:** Conceptualization, Formal analysis, manuscript revision. **Xiaojun Lian:** Conceptualization, manuscript revision. **Yong Wang:** Conceptualization, manuscript revision. **Yuguo Lei:** Conceptualization, experiment design, manuscript writing.

Declaration of competing interest

Authors have no competing financial interests.

Acknowledgments

This research was supported by the Nebraska DHHS Stem Cell Grant

2019 (YL), the Pennsylvania State University start-up (YL), and the University of Nebraska Collaboration Initiative Grant (YL, BD, SC).

Appendix A. Supplementary data

Supplementary data to this article can be found online at https://doi.org/10.1016/j.bioactmat.2022.10.022.

References

[1] M. Chan, Obesity and Diabetes: the Slow-Motion Disaster. Keynote Address at the 47th Meeting of the National Academy of Medicine, 1–7, World Heal. Organ., 2016. http://www.who.int/dg/speeches/2016/obesity-diabetes-disaster/en/.

[2] D.R. Leitner, G. Frühbeck, V. Yumuk, K. Schindler, D. Micic, E. Woodward, H. Toplak, Obesity and type 2 diabetes: two diseases with a need for combined treatment strategies - EASO can lead the way, Obes. Facts. 10 (2017) 483–492, https://doi.org/10.1159/000480525.

[3] N.L. Mihalopoulos, J.T. Yap, B. Beardmore, R. Holubkov, M.N. Nanjee, J. M. Hoffman, Cold-activated Brown adipose tissue is associated with less cardiometabolic dysfunction in young adults with obesity, Obesity 28 (2020) 916–923, https://doi.org/10.1002/oby.22767.

[4] C.T. Herz, O.C. Kulterer, M. Prager, C. Schmöltzer, F.B. Langer, G. Prager, R. Marculescu, A. Kautzky-Willer, M. Hacker, A.R. Haug, F.W. Kiefer, Active Brown adipose tissue is associated with a healthier metabolic phenotype in obesity, Diabetes 71 (2022) 93–103, https://doi.org/10.2337/db21-0475.

[5] A.G. Wibmer, T. Becher, M. Eljalby, A. Crane, P.C. Andrieu, C.S. Jiang, R. Vaughan, H. Schöder, P. Cohen, Brown adipose tissue is associated with healthier body fat distribution and metabolic benefits independent of regional adiposity, Cell Reports Med 2 (2021), https://doi.org/10.1016/j.xcrm.2021.100332.

[6] G.H.E.J. Vijgen, N.D. Bouvy, G.J.J. Teule, B. Brans, P. Schrauwen, W.D. van Marken Lichtenbelt, Brown adipose tissue in morbidly obese subjects, PLoS One 6 (2011) 2–7, https://doi.org/10.1371/journal.pone.0017247.

[7] M. Saito, Y. Okamatsu-Ogura, M. Matsushita, K. Watanabe, T. Yoneshiro, J. Nio-Kobayashi, T. Iwanaga, M. Miyagawa, T. Kameya, K. Nakada, Y. Kawai, M. Tsujisaki, High incidence of metabolically active brown adipose tissue in healthy adult humans: effects of cold exposure and adiposity, Diabetes 58 (2009) 1526–1531, https://doi.org/10.2337/db09-0530.

[8] T. Becher, S. Palanisamy, D.J. Kramer, M. Eljalby, S.J. Marx, A.G. Wibmer, S. D. Butler, C.S. Jiang, R. Vaughan, H. Schöder, A. Mark, P. Cohen, Brown adipose tissue is associated with cardiometabolic health, Nat. Med. 27 (2021) 58–65, https://doi.org/10.1038/s41591-020-1126-7.

[9] A.E. O'Mara, J.W. Johnson, J.D. Linderman, R.J. Brychta, S. McGehee, L. A. Fletcher, Y.A. Fink, D. Kapuria, T.M. Cassimatis, N. Kelsey, C. Cero, Z.A. Sater, F. Piccinini, A.S. Baskin, B.P. Leitner, H. Cai, C.M. Millo, W. Dieckmann, M. Walter, N.B. Javitt, Y. Rotman, P.J. Walter, M. Ader, R.N. Bergman, P. Herscovitch, K.Y. Chen, A.M. Cypess, Chronic mirabegron treatment increases human brown fat, HDL cholesterol, and insulin sensitivity, J. Clin. Invest. 130 (2020) 2209–2219, https://doi.org/10.1172/JCI131126.

[10] L.E. Ramage, M. Akyol, A.M. Fletcher, J. Forsythe, M. Nixon, R.N. Carter, E.J. R. van Beek, N.M. Morton, B.R. Walker, R.H. Stimson, Glucocorticoids acutely increase Brown adipose tissue activity in humans, revealing species-specific differences in UCP-1 regulation, Cell Metabol. 24 (2016) 130–141, https://doi.org/10.1016/j.cmet.2016.06.011.

[11] C. Yan, T. Zeng, K. Lee, M. Nobis, K. Loh, L. Gou, Z. Xia, Z. Gao, M. Bensellam, W. Hughes, J. Lau, L. Zhang, C.K. Ip, R. Enriquez, H. Gao, Q.P. Wang, Q. Wu, J. J. Haigh, D.R. Laybutt, P. Timpson, H. Herzog, Y.C. Shi, Peripheral-specific Y1 receptor antagonism increases thermogenesis and protects against diet-induced obesity, Nat. Commun. 12 (2021) 1–20, https://doi.org/10.1038/s41467-021-22925-3.

[12] M. Chondronikola, E. Volpi, E. Børsheim, C. Porter, P. Annamalai, S. Enerbäck, M. E. Lidell, M.K. Saraf, S.M. Labbe, N.M. Hurren, C. Yfanti, T. Chao, C.R. Andersen, F. Cesani, H. Hawkins, L.S. Sidossis, Brown adipose tissue improves whole-body glucose homeostasis and insulin sensitivity in humans, Diabetes 63 (2014) 4089–4099, https://doi.org/10.2337/db14-0746.

[13] A.A.J.J. Van Der Lans, J. Hoeks, B. Brans, G.H.E.J. Vijgen, M.G.W. Visser, M. J. Vosselman, J. Hansen, J.A. Jörgensen, J. Wu, F.M. Mottaghy, P. Schrauwen, W. D. Van Marken Lichtenbelt, Cold acclimation recruits human brown fat and increases nonshivering thermogenesis, J. Clin. Invest. 123 (2013) 3395–3403, https://doi.org/10.1172/JCI68993.

[14] P. Lee, S. Smith, J. Linderman, A.B. Courville, R.J. Brychta, W. Dieckmann, C. D. Werner, K.Y. Chen, F.S. Celi, Temperature-acclimated brown adipose tissue modulates insulin sensitivity in humans, Diabetes 63 (2014) 3686–3698, https://doi.org/10.2337/db14-0513.

[15] M.J.W. Hanssen, J. Hoeks, B. Brans, A.A.J.J. Van Der Lans, G. Schaart, J.J. Van Den Driessche, J.A. Jörgensen, M.V. Boekschoten, M.K.C. Hesselink, B. Havekes, S. Kersten, F.M. Mottaghy, W.D. Van Marken Lichtenbelt, P. Schrauwen, Short-term cold acclimation improves insulin sensitivity in patients with type 2 diabetes mellitus, Nat. Med. 21 (2015) 863–865, https://doi.org/10.1038/nm.3891.

[16] F. Villarroya, M. Giralt, The beneficial effects of brown fat transplantation: further evidence of an endocrine role of brown adipose tissue, Endocrinology 156 (2015) 2368–2370, https://doi.org/10.1210/en.2015-1423.

[17] M. Payab, M. Abedi, N. Foroughi Heravani, M. Hadavandkhani, M. Arabi, A. Tayanloo-Beik, M. Sheikh Hosseini, H. Gerami, F. Khatami, B. Larijani, M. Abdollahi, B. Arjmand, Brown adipose tissue transplantation as a novel alternative to obesity treatment: a systematic review, Int. J. Obes. 45 (2021) 109–121, https://doi.org/10.1038/s41366-020-0616-5.

[18] M.J. Betz, S. Enerbäck, Therapeutic prospects of metabolically active brown adipose tissue in humans, Front. Endocrinol. 2 (2011) 86, https://doi.org/10.3389/fendo.2011.00086.

[19] A. Kuryłowicz, M. Puzianowska-Kuźnicka, Induction of adipose tissue browning as a strategy to combat obesity, Int. J. Mol. Sci. 21 (2020) 1–28, https://doi.org/10.3390/ijms21176241.

[20] X. Liu, Z. Zheng, X. Zhu, M. Meng, L. Li, Y. Shen, Q. Chi, D. Wang, Z. Zhang, C. Li, Y. Li, Y. Xue, J.R. Speakman, W. Jin, Brown adipose tissue transplantation improves whole-body energy metabolism, Cell Res. 23 (2013) 851–854, https://doi.org/10.1038/cr.2013.64.

[21] Y. Liu, W. Fu, K. Seese, A. Yin, H. Yin, Ectopic brown adipose tissue formation within skeletal muscle after brown adipose progenitor cell transplant augments energy expenditure, Faseb. J. 33 (2019) 8822–8835, https://doi.org/10.1096/fj.201802162RR.

[22] X. Liu, S. Wang, Y. You, M. Meng, Z. Zheng, M. Dong, J. Lin, Q. Zhao, C. Zhang, X. Yuan, T. Hu, L. Liu, Y. Huang, L. Zhang, D. Wang, J. Zhan, H.J. Lee, J. R. Speakman, W. Jin, Brown adipose tissue transplantation reverses obesity in Ob/Ob mice, Endocrinology 156 (2015) 2461–2469, https://doi.org/10.1210/en.2014-1598.

[23] K.I. Stanford, R.J.W. Middelbeek, K.L. Townsend, D. An, E.B. Nygaard, K. M. Hitchcox, K.R. Markan, K. Nakano, M.F. Hirshman, Y.H. Tseng, L.J. Goodyear, Brown adipose tissue regulates glucose homeostasis and insulin sensitivity, J. Clin. Invest. 123 (2013) 215–223, https://doi.org/10.1172/JCI62308.

[24] S.C. Gunawardana, D.W. Piston, Insulin-independent reversal of type 1 diabetes in nonobese diabetic mice with brown adipose tissue transplant, Am. J. Physiol. Endocrinol. Metab. 308 (2015), E1043, https://doi.org/10.1152/ajpendo.00570.2014. E1055.

[25] K. Shankar, D. Kumar, S. Gupta, S. Varshney, S. Rajan, A. Srivastava, A. Gupta, A. P. Gupta, A.L. Vishwakarma, J.R. Gayen, A.N. Gaikwad, Role of brown adipose tissue in modulating adipose tissue inflammation and insulin resistance in high-fat diet fed mice, Eur. J. Pharmacol. 854 (2019) 354–364, https://doi.org/10.1016/j.ejphar.2019.02.044.

[26] L. Cheng, J. Wang, H. Dai, Y. Duan, Y. An, L. Shi, Y. Lv, H. Li, C. Wang, Q. Ma, Y. Li, P. Li, H. Du, B. Zhao, Brown and beige adipose tissue: a novel therapeutic strategy for obesity and type 2 diabetes mellitus, Adipocyte 10 (2021) 48–65, https://doi.org/10.1080/21623945.2020.1870060.

[27] X. Zhou, Z. Li, M. Qi, P. Zhao, Y. Duan, G. Yang, L. Yuan, Brown adipose tissue-derived exosomes mitigate the metabolic syndrome in high fat diet mice, Theranostics 10 (2020) 8197–8210, https://doi.org/10.7150/thno.43968.

[28] F. Villarroya, R. Cereijo, J. Villarroya, M. Giralt, Brown adipose tissue as a secretory organ, Nat. Rev. Endocrinol. 13 (2017) 26–35, https://doi.org/10.1038/nrendo.2016.136.

[29] M.W. Lee, M. Lee, K.J. Oh, Adipose tissue-derived signatures for obesity and type 2 diabetes: adipokines, batokines and microRNAs, J. Clin. Med. 8 (2019) 854, https://doi.org/10.3390/jcm8060854.

[30] J.D. White, R.S. Dewal, K.I. Stanford, The beneficial effects of brown adipose tissue transplantation, Mol. Aspect. Med. 68 (2019) 74–81, https://doi.org/10.1016/j.mam.2019.06.004.

[31] S.C. Gunawardana, D.W. Piston, Reversal of type 1 diabetes in mice by brown adipose tissue transplant, Diabetes 61 (2012) 674–682, https://doi.org/10.2337/db11-0510.

[32] R.K.C. Loh, B.A. Kingwell, A.L. Carey, Human brown adipose tissue as a target for obesity management; beyond cold-induced thermogenesis, Obes. Rev. 18 (2017) 1227–1242, https://doi.org/10.1111/obr.12584.

[33] R. Xue, M.D. Lynes, J.M. Dreyfuss, F. Shamsi, T.J. Schulz, H. Zhang, T.L. Huang, K.L. Townsend, Y. Li, H. Takahashi, L.S. Weiner, A.P. White, M.S. Lynes, L. L. Rubin, L.J. Goodyear, A.M. Cypess, Y.H. Tseng, Clonal analyses and gene profiling identify genetic biomarkers of the thermogenic potential of human brown and white preadipocytes, Nat. Med. 21 (2015) 760–768, https://doi.org/10.1038/nm.3881.

[34] C.H. Wang, M. Lundh, A. Fu, R. Kriszt, T.L. Huang, M.D. Lynes, L.O. Leiria, F. Shamsi, J. Darcy, B.P. Greenwood, N.R. Narain, V. Tolstikov, K.L. Smith, B. Emanuelli, Y.T. Chang, S. Hagen, N.N. Danial, M.A. Kiebish, Y.H. Tseng, CRISPR-engineered human brown-like adipocytes prevent diet-induced obesity and ameliorate metabolic syndrome in mice, Sci. Transl. Med. 12 (2020), https://doi.org/10.1126/SCITRANSLMED.AAZ8664.

[35] S. Carobbio, A.C. Guenantin, M. Bahri, S. Rodriguez-Fdez, F. Honig, I. Kamzolas, I. Samuelson, K. Long, S. Awad, D. Lukovic, S. Erceg, A. Bassett, S. Mendjan, L. Vallier, B.S. Rosen, D. Chiarugi, A. Vidal-Puig, Unraveling the developmental roadmap toward human Brown adipose tissue, Stem Cell Rep. 16 (2021) 641–655, https://doi.org/10.1016/j.stemcr.2021.01.013.

[36] L. Zhang, J. Avery, A. Yin, A.M. Singh, T.S. Cliff, H. Yin, S. Dalton, Generation of functional Brown adipocytes from human pluripotent stem cells via progression through a paraxial mesoderm state, Cell Stem Cell 27 (2020) 784–797, https://doi.org/10.1016/j.stem.2020.07.013.

[37] A.C. Brown, Brown adipocytes from induced pluripotent stem cells—how far have we come? Ann. N. Y. Acad. Sci. 1463 (2020) 9–22, https://doi.org/10.1111/nyas.14257.

[38] Oka, Kobayashi, Matsumura, Nishio, Saeki, Exogenous cytokine-free differentiation of human pluripotent stem cells into classical Brown adipocytes, Cells 8 (2019) 373, https://doi.org/10.3390/cells8040373.

[39] A.-L. Hafner, Human induced pluripotent stem cells: a new source for brown and white adipocytes, World J. Stem Cell. 6 (2014) 467, https://doi.org/10.4252/wjsc.v6.i4.467.
[40] K. Saeki, M. Nishio, T. Yoneshiro, M. Nakahara, S. Suzuki, K. Saeki, M. Hasegawa, Y. Kawai, H. Akutsu, A. Umezawa, K. Yasuda, K. Tobe, A. Yuo, K. Kubota, M. Saito, Production of functional classical brown adipocytes from human pluripotent stem cells using specific hemopoietin cocktail without gene transfer, Cell Metabol. 16 (2012) 394–406, https://doi.org/10.1016/j.cmet.2012.08.001.
[41] T. Ahfeldt, R.T. Schinzel, Y.K. Lee, D. Hendrickson, A. Kaplan, D.H. Lum, R. Camahort, F. Xia, J. Shay, E.P. Rhee, C.B. Clish, R.C. Deo, T. Shen, F.H. Lau, A. Cowley, G. Mowrer, H. Al-Siddiqi, M. Nahrendorf, K. Musunuru, R.E. Gerszten, J.L. Rinn, C.a. Cowan, Programming human pluripotent stem cells into white and brown adipocytes, Nat. Cell Biol. 14 (2012) 209–219, https://doi.org/10.1038/ncb2411.
[42] M. Nishio, K. Saeki, Differentiation of human pluripotent stem cells into highly functional classical brown adipocytes, Methods Enzymol. 537 (2014) 177–197, https://doi.org/10.1016/B978-0-12-411619-1.00010-0.
[43] A.L. Hafner, J. Contet, C. Ravaud, X. Yao, P. Villageois, K. Suknuntha, K. Annab, P. Peraldi, B. Binetruy, I.I. Slukvin, A. Ladoux, C. Dani, Brown-like adipose progenitors derived from human induced pluripotent stem cells: identification of critical pathways governing their adipogenic capacity, Sci. Rep. 6 (2016), 32490, https://doi.org/10.1038/srep32490.
[44] Y. Lei, D.V. Schaffer, A fully defined and scalable 3D culture system for human pluripotent stem cell expansion and differentiation, Proc. Natl. Acad. Sci. U.S.A. 110 (2013) E5039–E5048, https://doi.org/10.1073/pnas.1309408110.
[45] Q. Li, H. Lin, Q. Du, K. Liu, O. Wang, C. Evans, H. Christian, C. Zhang, Y. Lei, Scalable and physiologically relevant microenvironments for human pluripotent stem cell expansion and differentiation, Biofabrication 10 (2018), 025006, https://doi.org/10.1088/1758-5090/aaa6b5.
[46] H. Lin, Q. Li, O. Wang, J. Rauch, B. Harm, H.J. Viljoen, C. Zhang, E. Van Wyk, C. Zhang, Y. Lei, Automated expansion of primary human T cells in scalable and cell-friendly hydrogel microtubes for adoptive immunotherapy, Adv. Healthc. Mater. 7 (2018), 1701297, https://doi.org/10.1002/adhm.201701297.
[47] Y. Lei, D. Jeong, J. Xiao, D.V. Schaffer, Developing defined and scalable 3D culture systems for culturing human pluripotent stem cells at high densities, Cell. Mol. Bioeng. 7 (2014) 172–183, https://doi.org/10.1016/j.micinf.2011.07.011.Innate.
[48] Q. Li, Q. Wang, O. Wang, K. Shao, H. Lin, Y. Lei, A simple and scalable hydrogel-based system for culturing protein-producing cells, PLoS One 13 (2018), e0190364, https://doi.org/10.1371/journal.pone.0190364.
[49] H. Lin, Q. Li, Y. Lei, Three-dimensional tissues using human pluripotent stem cell spheroids as biofabrication building blocks, Biofabrication 9 (2017), 025007, https://doi.org/10.1088/1758-5090/aa663b.
[50] Q. Li, H. Lin, O. Wang, X. Qiu, S. Kidambi, L.P. Deleyrolle, B.A. Reynolds, Y. Lei, Scalable production of glioblastoma tumor-initiating cells in 3 dimension thermoreversible hydrogels, Sci. Rep. 6 (2016), 31951, https://doi.org/10.1038/srep31915.
[51] H. Lin, Q. Du, Q. Li, O. Wang, Z. Wang, N. Sahu, C. Elowsky, K. Liu, C. Zhang, S. Chung, B. Duan, Y. Lei, A scalable and efficient bioprocess for manufacturing human pluripotent stem cell-derived endothelial cells, Stem Cell Rep. 11 (2018) 454–469, https://doi.org/10.1016/j.stemcr.2018.07.001.
[52] H. Lin, Q. Li, Y. Lei, An integrated miniature bioprocessing for personalized human induced pluripotent stem cell expansion and differentiation into neural stem cells, Sci. Rep. 7 (2017), 40191, https://doi.org/10.1038/srep40191.
[53] J. Kim, M. Okla, A. Erickson, T. Carr, S.K. Natarajan, S. Chung, Eicosapentaenoic acid potentiates brown thermogenesis through FFAR4-dependent up-regulation of miR-30b and miR-378, J. Biol. Chem. 291 (2016) 20551–20562, https://doi.org/10.1074/jbc.M116.721480.
[54] G.L. Szot, P. Koudria, J.A. Bluestone, Transplantation of pancreatic islets into the kidney capsule of diabetic mice, JoVE (2007), https://doi.org/10.3791/404.
[55] T. Jofra, G. Galvani, F. Georgia, G. Silvia, N. Gagliani, M. Battaglia, Murine pancreatic islets transplantation under the kidney capsule, Bio-Protocol 8 (2018), e2743, https://doi.org/10.21769/bioprotoc.2743 e2743.
[56] M. Kuss, J. Kim, D. Qi, S. Wu, Y. Lei, S. Chung, B. Duan, Effects of tunable, 3D-bioprinted hydrogels on human brown adipocyte behavior and metabolic function, Acta Biomater. 71 (2018) 486–495, https://doi.org/10.1016/j.actbio.2018.03.021.
[57] T. Nishimura, T. Katsumura, M. Motoi, H. Oota, S. Watanuki, Experimental evidence reveals the UCP1 genotype changes the oxygen consumption attributed to non-shivering thermogenesis in humans, Sci. Rep. 7 (2017) 5570, https://doi.org/10.1038/s41598-017-05766-3.
[58] D. Ricquier, Uncoupling protein 1 of brown adipocytes, the only uncoupler: a historical perspective, Front. Endocrinol. 2 (2011) 85, https://doi.org/10.3389/fendo.2011.00085.
[59] S. Winer, Y. Chan, G. Paltser, D. Truong, H. Tsui, J. Bahrami, R. Dorfman, Y. Wang, J. Zielenski, F. Mastronardi, Y. Maezawa, D.J. Drucker, E. Engleman, D. Winer, H. Dosch, Normalization of obesity-associated insulin resistance through immunotherapy, Nat. Publ. Gr. 15 (2009) 921–930, https://doi.org/10.1038/nm.2001.
[60] Y.S. Lee, P. Li, J.Y. Huh, I.J. Hwang, M. Lu, J.I. Kim, M. Ham, S. Talukdar, A. Chen, W.J. Lu, G.K. Bandyopadhyay, R. Schwendener, J. Olefsky, J.B. Kim, Inflammation is necessary for long-term but not short-term high-fat diet-induced insulin resistance, Diabetes 60 (2011) 2474–2483, https://doi.org/10.2337/db11-0194.
[61] A. Gamble, R. Pawlick, A.R. Pepper, A. Bruni, A. Adesida, P.A. Senior, G. S. Korbutt, A.M.J. Shapiro, Improved islet recovery and efficacy through co-culture and co-transplantation of islets with human adipose-derived mesenchymal stem cells, PLoS One 13 (2018), e0206449, https://doi.org/10.1371/journal.pone.0206449.
[62] X. Zeng, M. Ye, J.M. Resch, M.P. Jedrychowski, B. Hu, B.B. Lowell, D.D. Ginty, B. M. Spiegelman, Innervation of thermogenic adipose tissue via a calsyntenin 3β–S100b axis, Nature 569 (2019) 229–235, https://doi.org/10.1038/s41586-019-1156-9.
[63] U.B. Pajvani, P.E. Scherer, Adiponectin: systemic contributor to insulin sensitivity, Curr. Diabetes Rep. 3 (2003) 207–213, https://doi.org/10.1007/s11892-003-0065-2.
[64] N. Maeda, I. Shimomura, K. Kishida, H. Nishizawa, M. Matsuda, H. Nagaretani, N. Furuyama, H. Kondo, M. Takahashi, Y. Arita, R. Komuro, N. Ouchi, S. Kihara, Y. Tochino, K. Okutomi, M. Horie, S. Takeda, T. Aoyamaa, T. Funahashi, Y. Matsuzawa, Diet-induced insulin resistance in mice lacking adiponectin/ACRP30, Nat. Med. 8 (2002) 731–737, https://doi.org/10.1038/nm724.
[65] M. Matsuda, I. Shimomura, M. Sata, Y. Arita, M. Nishida, N. Maeda, M. Kumada, Y. Okamoto, H. Nagaretani, H. Nishizawa, K. Kishida, R. Komuro, N. Ouchi, S. Kihara, R. Nagai, T. Funahashi, Y. Matsuzawa, Role of adiponectin in preventing vascular stenosis. The missing link of adipo-vascular axis, J. Biol. Chem. 277 (2002) 37487–37491, https://doi.org/10.1074/jbc.M206083200.
[66] S. Galic, J.S. Oakhill, G.R. Steinberg, Adipose tissue as an endocrine organ, Mol. Cell. Endocrinol. 316 (2010) 129–139, https://doi.org/10.1016/j.mce.2009.08.018.
[67] G. Fantuzzi, Adipose tissue, adipokines, and inflammation, J. Allergy Clin. Immunol. 115 (2005) 911–919, https://doi.org/10.1016/j.jaci.2005.02.023.
[68] G.X. Wang, X.Y. Zhao, J.D. Lin, The brown fat secretome: metabolic functions beyond thermogenesis, Trends Endocrinol. Metabol. 26 (2015) 231–237, https://doi.org/10.1016/j.tem.2015.03.002.
[69] K. Bozaoglu, K. Bolton, J. McMillan, P. Zimmet, J. Jowett, G. Collier, K. Walder, D. Segal, Chemerin is a novel adipokine associated with obesity and metabolic syndrome, Endocrinology 148 (2007) 4687–4694, https://doi.org/10.1210/en.2007-0175.
[70] C. Buechler, S. Feder, E.M. Haberl, C. Aslanidis, Chemerin isoforms and activity in obesity, Int. J. Mol. Sci. 20 (2019) 1128, https://doi.org/10.3390/ijms20051128.
[71] H. Yadav, S.G. Rane, TGF-β/Smad3 signaling regulates brown adipocyte induction in white adipose tissue, Front. Endocrinol. 3 (2012) 35, https://doi.org/10.3389/fendo.2012.00035.
[72] H. Yadav, C. Quijano, A.K. Kamaraju, O. Gavrilova, R. Malek, W. Chen, P. Zerfas, D. Zhigang, E.C. Wright, C. Stuelten, P. Sun, S. Lonning, M. Skarulis, A.E. Sumner, T. Finkel, S.G. Rane, Protection from obesity and diabetes by blockade of TGF-β/Smad3 signaling, Cell Metabol. 14 (2011) 67–79, https://doi.org/10.1016/j.cmet.2011.04.013.
[73] M.J. Jenkins, S.S. Farid, Human pluripotent stem cell-derived products: advances towards robust, scalable and cost-effective manufacturing strategies, Biotechnol. J. (2015), https://doi.org/10.1002/biot.201400348.
[74] C. Kropp, D. Massai, R. Zweigerdt, Progress and challenges in large-scale expansion of human pluripotent stem cells, Process Biochem. (2016) 1–11, https://doi.org/10.1016/j.procbio.2016.09.032, 10842.
[75] H. Kempf, B. Andree, R. Zweigerdt, Large-scale production of human pluripotent stem cell derived cardiomyocytes, Adv. Drug Deliv. Rev. 96 (2016) 18–30, https://doi.org/10.1016/j.addr.2015.11.016.
[76] M.M. Hunt, G. Meng, D.E. Rancourt, I.D. Gates, M.S. Kallos, Factorial experimental design for the culture of human embryonic stem cells as aggregates in stirred suspension bioreactors reveals the potential for interaction effects between bioprocess parameters, Tissue Eng. C Methods 20 (2014) 76–89, https://doi.org/10.1089/ten.tec.2013.0040.
[77] Z. Hajdu, V. Mironov, A.N. Mehesz, R.A. Norris, R.R. Markwald, R.P. Visconti, Tissue spheroid fusion-based in vitro screening assays for analysis of tissue maturation, J. Tissue Eng. Regen. Med. 4 (2010) 659–664, https://doi.org/10.1002/term.
[78] M. Serra, C. Correia, R. Malpique, C. Brito, J. Jensen, P. Bjorquist, M.J. T. Carrondo, P.M. Alves, Microencapsulation technology: a powerful tool for integrating expansion and cryopreservation of human embryonic stem cells, PLoS One 6 (2011), e23212, https://doi.org/10.1371/journal.pone.0023212.
[79] M. Chayosumrit, B. Tuch, K. Sidhu, Alginate microcapsule for propagation and directed differentiation of hESCs to definitive endoderm, Biomaterials 31 (2010) 505–514, https://doi.org/10.1016/j.biomaterials.2009.09.071.
[80] J. Stenberg, M. Elovsson, R. Strehl, E. Kilmare, J. Hyllner, A. Lindahl, Sustained embryoid body formation and culture in a non-laborious three dimensional culture system for human embryonic stem cells, Cytotechnology 63 (2011) 227–237, https://doi.org/10.1007/s10616-011-9344-y.
[81] S. Gerecht, J.A. Burdick, L.S. Ferreira, S.A. Townsend, R. Langer, G. Vunjak-Novakovic, Hyaluronic acid hydrogel for controlled self-renewal and differentiation of human embryonic stem cells, Proc. Natl. Acad. Sci. U.S.A. 104 (2007) 11298–11303, https://doi.org/10.1073/pnas.0703723104.
[82] H. Lin, Q. Li, Y. Lei, An integrated miniature bioprocessing for personalized human induced pluripotent stem cell expansion and differentiation into neural stem cells, Sci. Rep. 7 (2017), 40191, https://doi.org/10.1038/srep40191.
[83] H. Lin, Q. Du, Q. Li, O. Wang, Z. Wang, N. Sahu, C. Elowsky, K. Liu, C. Zhang, S. Chung, B. Duan, Y. Lei, A scalable and efficient bioprocess for manufacturing human pluripotent stem cell-derived endothelial cells, Stem Cell Rep. 11 (2018) 454–469, https://doi.org/10.1016/j.stemcr.2018.07.001.
[84] Z. Wang, F. Zuo, Q. Liu, X. Wu, Q. Du, Y. Lei, Z. Wu, H. Lin, Comparative study of human pluripotent stem cell-derived endothelial cells in hydrogel-based culture systems, ACS Omega 6 (2021) 6942–6952, https://doi.org/10.1021/acsomega.0c06187.

[85] H. Lin, Q. Du, Q. Li, O. Wang, Z. Wang, K. Liu, L. Akert, C. Zhang, S. Chung, B. Duan, Y. Lei, Differentiating human pluripotent stem cells into vascular smooth muscle cells in three dimensional thermoreversible hydrogels, Biomater. Sci. 7 (2019), https://doi.org/10.1039/c8bm01128a.
[86] Y. L, H. Lin, Q. Du, Q. Li, O. Wang, A scalable and efficient bioprocess for manufacturing human pluripotent stem cells-derived endothelial cells, Stem Cell Rep. 11 (2018) 454–469, https://doi.org/10.1016/j.stemcr.2018.07.001.
[87] J. Honek, S. Lim, C. Fischer, H. Iwamoto, T. Seki, Y. Cao, Brown adipose tissue, thermogenesis, angiogenesis: pathophysiological aspects, Horm. Mol. Biol. Clin. Invest. 19 (2014) 5–11, https://doi.org/10.1515/hmbci-2014-0014.
[88] Y. Cao, Angiogenesis and vascular functions in modulation of obesity, adipose metabolism, and insulin sensitivity, Cell Metabol. 18 (2013) 478–489, https://doi.org/10.1016/j.cmet.2013.08.008.
[89] M. Bagchi, L.A. Kim, J. Boucher, T.E. Walshe, C.R. Kahn, P.A. D'Amore, Vascular endothelial growth factor is important for brown adipose tissue development and maintenance, Faseb. J. 27 (2013) 3257–3271, https://doi.org/10.1096/fj.12-221812.
[90] I. Shimizu, T. Aprahamian, R. Kikuchi, A. Shimizu, K.N. Papanicolaou, S. MacLauchlan, S. Maruyama, K. Walsh, Vascular rarefaction mediates whitening of brown fat in obesity, J. Clin. Invest. 124 (2014) 2099–2112, https://doi.org/10.1172/JCI71643.
[91] K. Mahdaviani, D. Chess, Y. Wu, O. Shirihai, T.R. Aprahamian, Autocrine effect of vascular endothelial growth factor-A is essential for mitochondrial function in brown adipocytes, Metabolism 65 (2016) 26–35, https://doi.org/10.1016/j.metabol.2015.09.012.
[92] H. Lin, Q. Li, Q. Du, O. Wang, Z. Wang, L. Akert, M.A. Carlson, C. Zhang, A. Subramanian, C. Zhang, M. Lunning, M. Li, Y. Lei, Integrated generation of induced pluripotent stem cells in a low-cost device, Biomaterials 189 (2019) 23–36, https://doi.org/10.1016/j.biomaterials.2018.10.027.
[93] Q. Li, H. Lin, J. Rauch, L.P. Deleyrolle, B.A. Reynolds, H.J. Viljoen, C. Zhang, L. Gu, E. Van Wyk, Y. Lei, Scalable culturing of primary human glioblastoma tumor-initiating cells with a cell-friendly culture system, Sci. Rep. 8 (2018) 3531, https://doi.org/10.1038/s41598-018-21927-4.
[94] H. Lin, Q. Du, Q. Li, O. Wang, Z. Wang, K. Liu, C. Elowsky, C. Zhang, Y. Lei, Hydrogel-based bioprocess for scalable manufacturing of human pluripotent stem cell-derived neural stem cells, ACS Appl. Mater. Interfaces 10 (2018) 29238–29250, https://doi.org/10.1021/acsami.8b05780.
[95] H. Lin, Q. Du, Q. Li, O. Wang, Z. Wang, C. Elowsky, K. Liu, C. Zhang, S. Chung, B. Duan, Y. Lei, Manufacturing human pluripotent stem cell derived endothelial cells in scalable and cell-friendly microenvironments, Biomater. Sci. 7 (2019) 373–388, https://doi.org/10.1039/c8bm01095a.
[96] H. Lin, X. Qiu, Q. Du, Q. Li, O. Wang, L. Akert, Z. Wang, D. Anderson, K. Liu, L. Gu, C. Zhang, Y. Lei, Engineered microenvironment for manufacturing human pluripotent stem cell-derived vascular smooth muscle cells, Stem Cell Rep. 12 (2019) 84–97, https://doi.org/10.1016/j.stemcr.2018.11.009.
[97] O. Wang, Y. Lei, Creating a cell-friendly microenvironment to enhance cell culture efficiency, Cell Gene Ther. Insights. 5 (2019) 341–350, https://doi.org/10.18609/cgti.2019.038.
[98] P. Trayhurn, S.Y. Alomar, Oxygen deprivation and the cellular response to hypoxia in adipocytes - perspectives on white and brown adipose tissues in obesity, Front. Endocrinol. 6 (2015) 19, https://doi.org/10.3389/fendo.2015.00019.
[99] K. Sun, C.M. Kusminski, K. Luby-Phelps, S.B. Spurgin, Y.A. An, Q.A. Wang, W. L. Holland, P.E. Scherer, Brown adipose tissue derived VEGF-A modulates cold tolerance and energy expenditure, Mol. Metabol. 3 (2014) 474–483, https://doi.org/10.1016/j.molmet.2014.03.010.
[100] C.H. Wang, M. Lundh, A. Fu, R. Kriszt, T.L. Huang, M.D. Lynes, L.O. Leiria, F. Shamsi, J. Darcy, B.P. Greenwood, N.R. Narain, V. Tolstikov, K.L. Smith, B. Emanuelli, Y.T. Chang, S. Hagen, N.N. Danial, M.A. Kiebish, Y.H. Tseng, CRISPR-engineered human brown-like adipocytes prevent diet-induced obesity and ameliorate metabolic syndrome in mice, Sci. Transl. Med. 12 (2020), https://doi.org/10.1126/SCITRANSLMED.AAZ8664.
[101] Y. Shi, H. Inoue, J.C. Wu, S. Yamanaka, Induced pluripotent stem cell technology: a decade of progress, Nat. Rev. Drug Discov. 16 (2017) 115–130, https://doi.org/10.1038/nrd.2016.245.
[102] K. Takahashi, K. Tanabe, M. Ohnuki, M. Narita, T. Ichisaka, K. Tomoda, S. Yamanaka, Induction of pluripotent stem cells from adult human fibroblasts by defined factors, Cell 131 (2007) 861–872, https://doi.org/10.1016/j.cell.2007.11.019.
[103] K. Okita, Y. Matsumura, Y. Sato, A. Okada, A. Morizane, S. Okamoto, H. Hong, M. Nakagawa, K. Tanabe, K. Tezuka, T. Shibata, T. Kunisada, M. Takahashi, J. Takahashi, H. Saji, S. Yamanaka, A more efficient method to generate integration-free human iPS cells, Nat. Methods 8 (2011) 409–412, https://doi.org/10.1038/nmeth.1591.
[104] R. Araki, M. Uda, Y. Hoki, M. Sunayama, M. Nakamura, S. Ando, M. Sugiura, H. Ideno, A. Shimada, A. Nifuji, M. Abe, Negligible immunogenicity of terminally differentiated cells derived from induced pluripotent or embryonic stem cells, Nature 494 (2013) 100–104, https://doi.org/10.1038/nature11807.
[105] M. Mandai, A. Watanabe, Y. Kurimoto, Y. Hirami, C. Morinaga, T. Daimon, M. Fujihara, H. Akimaru, N. Sakai, Y. Shibata, M. Terada, Y. Nomiya, S. Tanishima, M. Nakamura, H. Kamao, S. Sugita, A. Onishi, T. Ito, K. Fujita, S. Kawamata, M.J. Go, C. Shinohara, K. Hata, M. Sawada, M. Yamamoto, S. Ohta, Y. Ohara, K. Yoshida, J. Kuwahara, Y. Kitano, N. Amano, M. Umekage, F. Kitaoka, A. Tanaka, C. Okada, N. Takasu, S. Ogawa, S. Yamanaka, M. Takahashi, Autologous induced stem-cell–derived retinal cells for macular degeneration, N. Engl. J. Med. 376 (2017) 1038–1046, https://doi.org/10.1056/nejmoa1608368.
[106] W. Zhao, A. Lei, L. Tian, X. Wang, C. Correia, T. Weiskittel, H. Li, A. Trounson, Q. Fu, K. Yao, J. Zhang, Strategies for genetically engineering hypoimmunogenic universal pluripotent stem cells, iScience 23 (2020), 101162, https://doi.org/10.1016/j.isci.2020.101162.
[107] X. Han, M. Wang, S. Duan, P.J. Franco, J.H.R. Kenty, P. Hedrick, Y. Xia, A. Allen, L.M.R. Ferreira, J.L. Strominger, D.A. Melton, T.B. Meissner, C.A. Cowan, Generation of hypoimmunogenic human pluripotent stem cells, Proc. Natl. Acad. Sci. U.S.A. 116 (2019) 10441–10446, https://doi.org/10.1073/pnas.1902566116.
[108] T. Deuse, X. Hu, A. Gravina, D. Wang, G. Tediashvili, C. De, W.O. Thayer, A. Wahl, J.V. Garcia, H. Reichenspurner, M.M. Davis, L.L. Lanier, S. Schrepfer, Hypoimmunogenic derivatives of induced pluripotent stem cells evade immune rejection in fully immunocompetent allogeneic recipients, Nat. Biotechnol. 37 (2019) 252–258, https://doi.org/10.1038/s41587-019-0016-3.
[109] H.R. Frederiksen, U. Doehn, P. Tveden-Nyborg, K.K. Freude, Non-immunogenic induced pluripotent stem cells, a promising way forward for allogenic transplantations for neurological disorders, Front. Genome Ed. 2 (2021), https://doi.org/10.3389/fgeed.2020.623717.